



NKS-434  
ISBN 978-87-7893-524-3

---

Corrosion of copper in sulphide containing environment:  
the role and properties of sulphide films –  
Annual report 2019

Vilma Ratia<sup>1</sup>, Leena Carpén<sup>1</sup>, Elisa Isotahdon<sup>1</sup>

Cem Örnek<sup>2</sup>, Fan Zhang<sup>2</sup>, Jinshan Pan<sup>2</sup>

<sup>1</sup>VTT Technical Research Centre of Finland Ltd., Espoo, Finland

<sup>2</sup>KTH Royal Institute of Technology, Stockholm, Sweden

April 2020

## Abstract

OFP-copper samples were exposed to anoxic simulated groundwater with varying amounts of sulphide addition (0-640 mg/L) to study the effect of the presence of sulphides in simulated repository conditions. Copper samples in two states were used: in ground/polished state and pre-oxidised state (7 days, 90 °C in air). The duration of exposure was 4 months in these experiments, to get initial results aiding the selection of experimental parameters for the longer term experiments later. In addition to this, an experiment with the exposure duration of 2 months was conducted. Several characterisation methods were used: visual examination, scanning electron microscopy and energy dispersive X-ray spectroscopy, scanning Kelvin probe force microscopy and high-energy X-ray diffraction. Moreover, electrochemical data was collected throughout the experiment.

The results indicate that the addition of sulphide in the simulated groundwater has a distinct effect on copper. The surfaces were affected already at the lowest addition level (3 mg/L), however there was local variance in the surfaces. The electrochemical measurements suggested that the corrosion was the highest with higher sulphide addition (320 mg/L was the highest electrochemically measured sample). Open circuit potentials of the samples were the lower, the higher the addition of sulphide was.

Main preliminary conclusion from the synchrotron XRD measurement was that in addition to the copper sulfide compounds formed on the surface, the exposure also induced the structural change of the surface region of copper, which may increase the susceptibility to cracking under mechanical stress. Further measurement and analysis of H and S ingress into the copper are needed to draw a safe conclusion.

The water measurements indicated that there may be a reaction between the simulated groundwater with added sulphide and the vessel, and this needs to be considered before the next experiment. As the next steps, the longer term experiments are set up, and the further/more detailed characterisation of the samples continues.

## Key words

corrosion, copper, nuclear waste, sulphide, characterisation

NKS-434  
ISBN 978-87-7893-524-3  
Electronic report, April 2020  
NKS Secretariat  
P.O. Box 49  
DK - 4000 Roskilde, Denmark  
Phone +45 4677 4041  
[www.nks.org](http://www.nks.org)  
e-mail [nks@nks.org](mailto:nks@nks.org)

# **Corrosion of copper in sulphide containing environment: the role and properties of sulphide films - Annual report 2019**

**Final Report from the NKS-R COCOS (Contract: AFT/NKS-R(19)127/2)**

Vilma Ratia<sup>1</sup>, Leena Carpén<sup>1</sup>, Elisa Isotahdon<sup>1</sup>  
Cem Örneke<sup>2</sup>, Fan Zhang<sup>2</sup>, Jinshan Pan<sup>2</sup>

<sup>1</sup>VTT Technical Research Centre of Finland Ltd., Espoo, Finland

<sup>2</sup>KTH Royal Institute of Technology, Stockholm, Sweden

## Table of contents

	Page
1. Introduction	4
2. Real-time electrochemical monitoring of copper corrosion rate at the underground nuclear waste condition – literature review	4
2.1 Corrosion during the oxic period	6
2.1.1 Real-time corrosion monitoring at Äspö	6
2.1.2 General corrosion rate monitoring	7
2.1.3 Localized corrosion prediction	8
2.2 Microbial corrosion	8
2.2.1 In anoxic groundwater	8
2.2.1.1 With sulphate-reducing bacteria and methanogens	9
2.2.1.2 With sulphate-reducing bacteria only	9
2.2.1.3 Time dependence of microbial corrosion	9
2.2.2 In oxic groundwater	9
2.3 Sulphide induced corrosion	9
2.4 Literature review summary	11
3. Materials and methods	11
3.1 Materials	11
3.2 Exposure conditions	12
3.3 Methods	12
3.3.1 Electrochemical methods	12
3.3.2 Microscopy	13
3.3.3 Water chemistry measurements	13
3.3.4 High-energy X-ray diffraction (HEXRD)	13
3.3.5 Scanning Kelvin probe force microscopy (SKPFM)	14
4. Results and discussion	14
4.1 Electrochemical measurements	14
4.2 Surface characterisation: 2 month tests	15
4.2.1 Visual observations	15
4.2.2 SEM observations	16
4.2.3 Scanning Kelvin probe force microscopy	18
4.2.4 High-energy X-ray diffraction	19

4.3 Surface characterisation: 4 month tests	20
4.3.1 Visual observations	20
4.3.2 SEM observations	22
4.4 Water analysis	24
4.4.1 Proposition for further tests to find the source of additional silicon and boron	26
4.5 Selecting the parameters for the next experiments	27
5 Summary and conclusions	29
Acknowledgments	29
Disclaimer	30
6 References	30

## 1. Introduction

This is the annual report for the year 2019 for project COCOS, in which the corrosion of copper in sulphide containing environment is studied. The project's aim is to characterise the role and properties of sulphide films on copper.

The nuclear waste disposal concept in Finland and Sweden, called KBS-3 (Bennett & Gens, 2008), is based on a multi-barrier system. In this system, the spent nuclear fuel is placed in cast iron containers, which are then sealed in copper canisters. The copper canisters are further placed in holes drilled into deep bedrock, and the holes are finally filled with bentonite clay. It is expected that the bentonite clay provides a favourable environment for the copper canisters to retain their integrity for at least 100 000 years. However, an open question was raised by The Land and Environment Court in Sweden concerning the long-term safety of copper canister in sulphidic environment. Indeed, the deep bedrock in Fennoscandian area is very sulphidic due to, for example, presence of pyrite ( $\text{FeS}_2$ ), and sulphide included in the groundwater in small amounts. An important issue is that the near-environment of canisters is supposed to contain plenty of sulphate, not only in the ground water but also in the bentonite clay, and sulphate reducing bacteria (SRB) that thrive under the anoxic conditions in the groundwater surroundings easily metabolize sulphates into sulphides. Therefore, there may be a direct contact with the copper canister and a sulphide-containing environment during the repository time scale.

According to previous studies, the sulphide species are known to cause the formation of barrier layer on copper (Carpén et al., 2018; Chen et al., 2010; Huttunen-Saarivirta et al., 2016; Huttunen-Saarivirta et al. 2017a). The long-term strength of the layer is a question that requires further research. The main characteristics of the barrier layer are determined by sulphide concentration together with the presence and concentration of aggressive ions, such as chlorides (Mao et al., 2014). Thus, sulphide species has a strong influence on the overall lifetime of the canister and the tendency of copper canisters for localized corrosion damage in the repository. However, at present there is not enough scientific knowledge on how copper behaves at various expected sulphide contents and in varying conditions of the repository environment, and this is where the COCOS project steps in.

This report, being the first annual report, describes results obtained from the first experiments and it has been done through the collaboration between VTT Technical Research Centre of Finland Ltd. and KTH Royal Institute of Technology, Sweden. The report contains a review section (by Fan Zhang, second chapter) and then progresses to the description of the current experimental details and results, as well as discussion on the selection of parameters for the next experiments.

## 2. Real-time electrochemical monitoring of copper corrosion rate at the underground nuclear waste condition – literature review

A large amount of spent fuel is produced every year from large-scale commercial nuclear power plants, which contains about 1% of highly radioactive compounds of  $^{235}\text{U}$  and Pu, the actinides and other long-life fission products. These compounds may leave severe environmental pollution if mishandled. Therefore, the safe disposal of nuclear waste is an issue as important as nuclear safety. So far, those produced high-level radioactive wastes are currently being stored underwater in special ponds or in dry concrete structures or casks, which are considered as no permanent disposal method.

The geological disposal is the commonly accepted approach for the permanent disposal of used nuclear fuel and wastes, by which a high-level radioactive waste containing repository will be placed in deep rocks at 500 to 1000 m underground, to achieve isolation of human living environment at least greater than 100,000 years (Wang Ju, 2003). The concept relies on the containment and retention effects of both engineering barrier and geological barrier. The engineering barrier consists of the buffer backfill material of wastes, waste tank and the external package. Whereas, the geological barrier consists of rocks (granite, clay, tuff or rock salt, etc.) and geological bodies surrounding the engineering barrier. Therefore, the corrosion resistance and time-dependent characteristics of the storage container are of the utmost importance to ensure the sealing of nuclear wastes and prevent/retard their releasing into the human living in the environment.

There are two strategies that can be applied for the container material selection to avoid corrosion-related failures. The first one is using corrosion-resistant materials. The second option is using corrosion-allowance materials at a sufficient thickness for corrosion penetration, having predictable corrosion rate and no localized corrosion behaviours (Kursten et al., 2004).

A wide variety of metallic materials have been investigated as candidates for making containers, such as carbon steel (Foct & Gras, 2003), stainless steels (Sridhar and Cragolino, 1993), Ni alloys (Cragolino & Sridhar, 1991; Cragolino et al., 2011), Ti alloys (Shoesmith et al., 1994) (Ikeda et al., 1994) and Cu alloys. In Sweden and Finland, the major effort was directed on copper (DoE, 2002). Copper has presented its advantages on aspects of economic and corrosion resistant. Chinese archaeological data indicate that the excavated bronze relics can well stand for over 3,000 years. Copper is one of the thermodynamically stable materials in reducing conditions free of complexing agents (Hedman et al., 2002). Sweden is at the forefront at the construction of high-level radioactive permanent storage project, and has established the nuclear waste storage with pure copper with a thickness of 5 cm. In Finland, the final disposal of high-level radioactive waste is planned to begin already in the year 2020 (Hellä et al., 2014). During the geological disposal process, oxygen exists in the initial period of the repository closure lasting tens to hundreds of years, and is consumed by oxidation reactions and microorganisms. Then, sulphides from sulphate-reducing bacteria, mineral decomposition and groundwater will act as the only oxidant for the copper container. Meanwhile, the chlorides in the environment may also affect the corrosion behaviour of copper (Scully & Edwards, 2013).

Prediction of the lifetime of the nuclear waste disposal construction is challenging due to the long timescales of the expected service time and requirement of a sound mechanistic understanding of the corrosion processes of the materials (King & Kolar, 2018). Considerable efforts have been made to investigate the corrosion and monitor the corrosion rate of copper in repository-related environments over the past 40 years. The researches include (i) general and localized corrosion in the early oxidizing period, (ii) general corrosion in oxygen-free conditions with and without  $\text{SH}^-$ .

Moreover, in situ corrosion rate monitoring is crucial both to demonstrate the feasibility of a repository construction and operation, and to build confidence in the performance. However, in most of the reported work, the lifetime prediction of copper containers was extrapolated from relatively short-term experimental data (He et al., 2017). A few works involve long term

tests with corrosion coupons, and sometimes full-scale containers exposed to realistic disposal conditions for periods up to 20 months providing the valuable in situ and long-term corrosion data in representative settings that would not be available from laboratory studies (Smart et al., 2017).

In both Sweden and Finland, the geological repository is the principal strategy for high-level radioactive waste disposal. Copper is chosen as the canister material due to its promising corrosion resistance in the anoxic solution. The tightly sealed canisters containing the solid spent nuclear fuel are enclosed by the bentonite clay and embedded in rock at the depth of about 500 m below the sea level. The research groups of this project from both Sweden and Finland have conducted a range of work using electrochemical methods to in situ monitor the real-time corrosion rate of copper exposed at nuclear waste relevant environments, and explored the mechanisms beneath. With the highest relevance of the ongoing collaborative project, this report mainly reviews the work from the two groups of KTH and VTT. The studies from KTH are primarily focused on the long-term corrosion behaviour of copper with focus on the oxic period after emplacement, and from VTT are mainly focused on the microbial corrosion of copper in the repository system.

## **2.1 Corrosion during the oxic period**

Initially, a limited amount of air will be left in a repository after emplacement. The entrapped oxygen will be consumed through reactions with minerals in the rock and the bentonite, as well as through microbial activity. After the oxygen has been consumed in the repository, after a few hundred years at the very most, corrosion will be controlled completely by the supply of dissolved sulphide to the canister. The initial oxic period is considered the most harmful, when considering the risk of localization of the corrosion attack. To address the challenge to arrange final storage for the nuclear waste ‘in an absolutely safe way’ with a life of a hundred thousand to a million years, the research group from KTH has carried out extensive researches to monitor the corrosion rate of the copper canister in the oxic period.

### **2.1.1 Real-time corrosion monitoring at Äspö**

It is essential to ascertain a proper near-field environment for the corrosion test of the copper canister. As illustrated in Figure 1, the Äspö Hard Rock Laboratory offers a realistic environment for different experiments and tests under the conditions that will prevail in a deep repository (Andersson et al., 2004). The real-time monitoring of copper corrosion can be performed and combined with back-up studies for better understanding and evaluation. Copper coupons are exposed in the ‘Long Term Test of Buffer Material’ (LOT) test parcels, which gives information about average corrosion rates, type of corrosion attack and corrosion products (Karlund & Sandén, 1999).

Several electrochemical, electric resistance probes are available for real-time corrosion monitoring, which comprise polarization resistance, harmonic distortion analysis, electrode impedance spectroscopy, and electrochemical noise techniques. For the real-time corrosion monitoring, a commercially available SmartCET corrosion monitoring system using a three-electrode set-up has been used (Bo et al., 2005). The electrochemical real-time monitoring techniques offer the best sensitivity and give instantaneous information.

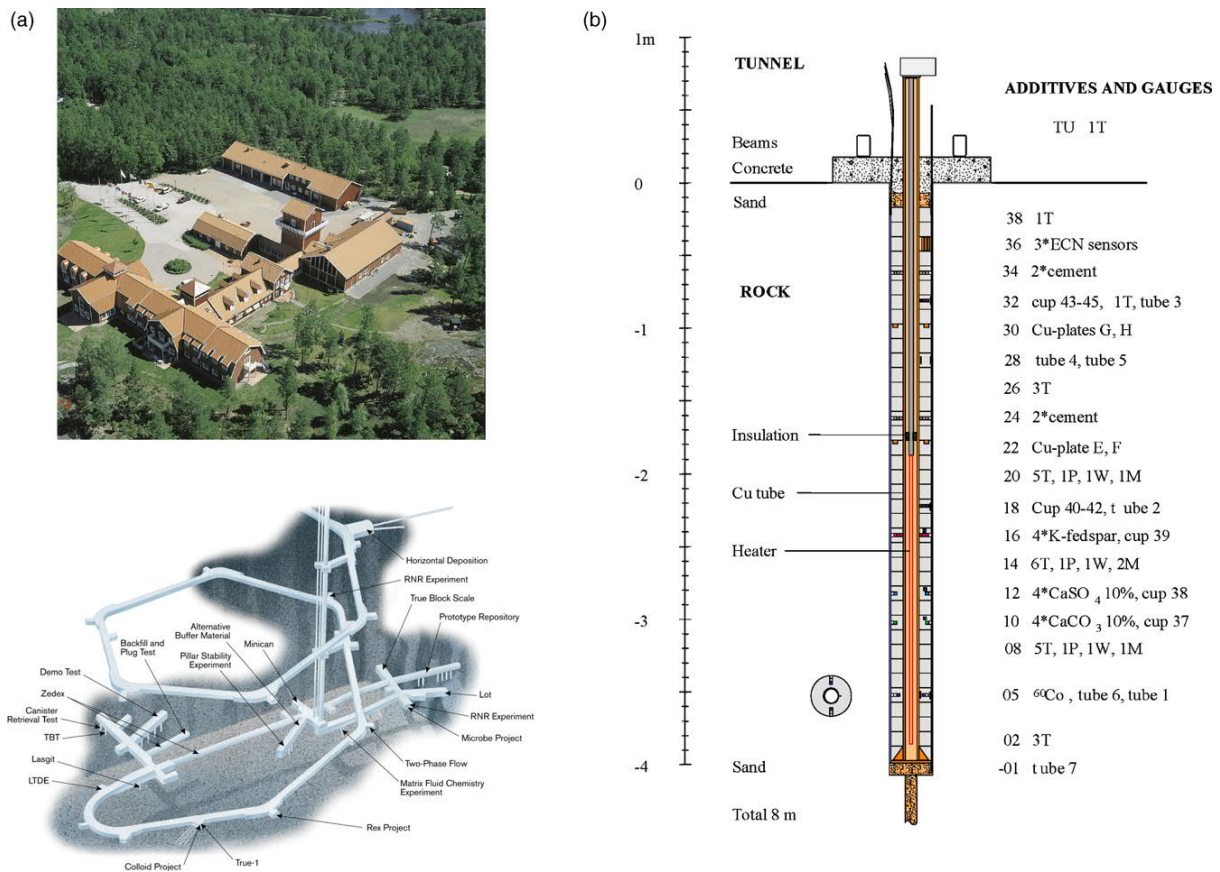


**Figure 1.** (a) View of the Äspö Hard Rock Laboratory above and below ground and (b) the bentonite test parcel. (Bo and Pan, 2008)

### 2.1.2 General corrosion rate monitoring

Up to six years of exposure has been made to investigate corrosion behaviour of copper electrodes in LOT test parcel or prototype repository, and these measurements are supported with back-up experiments to validate the understanding of corrosion mechanisms.

The copper samples present very low instantaneous corrosion rates in both LOT and prototype repository tests (Rosborg et al., 2003; Rosborg et al., 2004; Bo et al., 2005), even given the fact, the electrochemical techniques seem to overestimate the corrosion rate (Bo et al., 2005). The overestimated corrosion rates are mainly because of the overall ‘electrochemical activity’ is measured but a redox reaction shields the actual corrosion rate (Bo et al., 2005). Alternatively, both the anodic and cathodic reactions are under charge-transfer control, and the corrosion rate is merely overestimated by not using a sufficiently low measuring frequency to obtain the true polarization resistance. The results from the measurements with the electric resistance probes are supposed to clarify this.

The corrosion resistance of pure copper in this environment mainly depends on a thin protective cuprite film that forms readily, and on a thick porous outer corrosion product layer (mainly cuprite) that develops slowly and partly intermixes with the bentonite (Bo & Pan, 2008). The pre-exposed copper electrodes were greatly disturbed during retrieval of the LOT test parcel, which causes a major change in the corrosion rates and corrosion potentials (Bo & Pan, 2008). The retrieval-induced distribution takes a few months until the copper electrodes return to the low and steady-state corrosion rates, but the recorded corrosion rates are

somewhat higher even long after retrieval. The phenomena can be explained by the bentonite and its swelling pressure contribute favourably to the corrosion resistance of copper in the bentonite/saline groundwater environment by means of improving the adherence of the cuprite layer, and maybe even decreasing the porosity of the outer cuprite layer on the copper surface.

Results from 3 years simulated laboratory test reveal decreasing but measurable corrosion rates all through the exposure, and the corrosion resistance of copper is improved by the presence of bentonite (Bo et al., 2011).

### **2.1.3 Localized corrosion prediction**

Pilot efforts with real-time monitoring of localized corrosion are performed at the Äspö with back-up laboratory work at KTH in Stockholm (Rosborg et al., 2004). The recorded results indicate a tendency of localized attack, but an inability to maintain the attack. The copper coupons from the retrieved test parcels have a somewhat uneven corrosion attack with different corrosion products on the surfaces, but no obvious signs of pitting (Rosborg et al., 2004).

## **2.2 Microbial corrosion**

The rocks are stable and durable providing the outmost barrier of the multi-barrier structure between the fuel and the biosphere. The bentonite clay acts as a barrier separating groundwater and the canisters, buffering minor movements of the repository system, and retaining the eventual release of nuclides upon copper canister failure. Even with such rigorous protection, canister still may get into contact with groundwater and microbes, in the cases of uneven saturation and swelling of the bentonite or formation of water-bearing fractures. The colonization and activity of microbes on the surface or in the vicinity of the canister may initiate and accelerate several corrosion mechanisms including general or localized corrosion, galvanic corrosion, and intergranular corrosion, as well as enable stress-corrosion cracking (Carpén et al., 2017). Microbial metabolites can affect the corrosion processes by means of altering pH and redox potential, excreting corrosion-inducing metabolites, enzymatic reducing or oxidizing the corrosion products, and forming biofilms that create corrosive microenvironments. The processes and mechanisms are complex and challenging but of great importance for validating the long-term safety of nuclear waste disposal concept. To address the challenges, the research group from VTT have made throughout investigation on how microbes affect the corrosion behaviour and corrosion resistance of the copper in the geological repository simulating environments. A range of electrochemical and gravimetric measurements has been applied, and electric resistance (ER) probes, the physical method is suggested to be the most sensitive tool for monitoring initial corrosion of copper and gives the most conservative estimation of the lifetime (Marja-aho et al., 2018).

### **2.2.1 In anoxic groundwater**

Studies have been first carried out in the laboratory condition simulating the final stage of the deep geological nuclear waste repository, when the temperature has already stabilized to the level of the surrounding bedrock and where all oxygen introduced at the construction stage has been consumed. Copper samples were in direct contact with the groundwater, simulating the scenario where bentonite buffer has lost its full performance. The chemistry of artificial groundwater was designed to simulate the groundwater of the repository, which had been stabilized with bentonite. Sulphate-reducing bacteria (SRB) and methanogens are the species

found to be enriched in the repository environment. It has been demonstrated that the species of microorganisms affect the deposit formation on the surface of copper and the form corrosion (Carpén et al., 2018).

#### **2.2.1.1 With sulphate-reducing bacteria and methanogens**

Upon the presenting of both microbes, full coverage of spongy sulphur-containing deposit layer forms and loosely attaches to the copper oxide film (Carpén et al., 2017). Results from shorter (4.7 months) exposures show that the corrosion rate in the biotic environment was clearly smaller than in abiotic environment (Carpén et al., 2016). Whereas, results from one-year exposure suggest that the biofilm does not affect the corrosion rate of copper significantly but increases the dissolution rate of copper (Carpén et al., 2017).

#### **2.2.1.2 With sulphate-reducing bacteria only**

On the other hand, in the similar artificial groundwater but only inoculated SRB, the corrosion rate is clearly accelerated by the bacteria (Huttunen-Saarivirta et al., 2016), and SRB can form a dense biofilm on the copper surfaces (Carpén et al., 2018). In this condition, the deposition of biotically produced  $\text{Cu}_2\text{S}$  layer is detected above the general corrosion sites. The formation and properties of the  $\text{Cu}_2\text{S}$  layer are regulated by the growth of the biofilm (Huttunen-Saarivirta et al., 2016). Within 4 months of exposure, the OCP is higher in biotic condition than that of abiotic system, and both general and localized corrosion events can be detected on the copper surface. However, 10 months experimental results show that the formed  $\text{Cu}_2\text{S}$  layer is corrosion protective, only general corrosion attack occurs in biotic condition (Huttunen-Saarivirta et al., 2016; Carpén et al., 2018). This biotically induced protective  $\text{Cu}_2\text{S}$  layer presents a typical character of the p-type semiconductor, which shows a higher diffusion constant for cation vacancies the average bulk cation vacancy concentration in the barrier layer than electrochemically developed  $\text{Cu}_2\text{S}$  layers (Huttunen-Saarivirta et al., 2018).

#### **2.2.1.3 Time dependence of microbial corrosion**

To clarify the mechanisms of the time dependence of the biotically induced electrochemical property, the effort has been made to identify majority microbial species in the biofilm after different exposure time, which is important for successful prediction of the behaviour of copper (Huttunen-Saarivirta et al., 2017a). In the 4-month test, the Alphaproteo bacteria (Rhizobiales) are dominating in the biofilm where the highest corrosion rate has been observed. In the 10-month test, however, Deltaproteobacteria (i.a. SRB) is the majority in the biofilm providing the low corrosion rate of the copper. The results further confirm that the presence of microorganisms such as SRB may enhance the passivity of copper.

#### **2.2.2 In oxic groundwater**

As one of the very few contributions, the research group of VTT has also studied the microbial corrosion of copper under oxidizing conditions (Huttunen-Saarivirta et al., 2017b). Long-term immersion experiments have been performed to simulate the initial oxic stage of the deep geological nuclear waste repository in the presence of bentonite. The key finding of the study is the presence of oxygen and the high concentration of calcium of the groundwater, play a more important role in the corrosion behaviour of copper than the presence of bacteria.

#### **2.3 Sulphide induced corrosion**

Once oxygen, trapped in the repository on sealing, the major threat to the long-term durability of the copper container is corrosion by sulphide ( $\text{SH}^-$ ) produced in the groundwater by

mineral dissolution and/or microbial activity involving sulphate-reducing bacteria (King et al., 2010; Pedersen, 2000).

Given the fact that, in the real repository conditions, the copper surface has been oxidised into prior to contact with water since it is kept in the atmosphere before its placement in the final repository. Oxidation of Cu can result in a partially protective  $\text{Cu}_2\text{O}$  film, or a film consists of a porous base  $\text{Cu}_2\text{O}$  layer and an outer  $\text{CuO}$  /  $\text{Cu}(\text{OH})_2$  layer. The surface oxides can be converted into sulphides at a rate dependent on oxide film thickness and sulphide concentration. The conversion goes to completion with extends relatively deep into the bulk material (Hollmark et al., 2012; Smith et al., 2007).

Moreover, the presence of sulphide will lead to the formation of  $\text{Cu}_2\text{S}$  on the corroding Cu surface, in the way the dissociation of  $\text{SH}^-$  supplies protons and drive the corrosion reaction (Chen et al., 2011; Kong et al., 2017). The  $\text{Cu}_2\text{S}$  is found to be present as a chalcocite ( $\text{Cu}_2\text{S}$ )/digenite ( $\text{Cu}_{1.8}\text{S}$ ) deposition film a Cu surface in anaerobic sulphide solutions, the properties of which not only depend on the concentration of  $\text{SH}^-$  and  $\text{Cl}^-$ , but also their ratio (Chen et al., 2014; Martino et al., 2017). Efforts have been made to clarify the role of  $\text{Cl}^-$  and  $\text{SH}^-$  on the formation of the  $\text{Cu}_2\text{S}$  films and their corrosion behaviour.

In agreement with long-term corrosion results under natural corrosion conditions, investigation under electrochemical polarisation conditions demonstrates that, when the film growth is dominated by sulphide diffusion in solution, a single layer porous  $\text{Cu}_2\text{S}$  film or a dual-layer  $\text{Cu}_2\text{S}$  film forms, whereas if film growth is controlled by an interfacial reaction, a compact partially passivating film forms (Martino et al., 2014). Moreover, the  $\text{Cu}_2\text{S}$  film growth occurs at the  $\text{Cu}_2\text{S}$ /electrolyte interface, and its kinetics in anoxic conditions is parabolic and controlled by the Cu diffusion in porous  $\text{Cu}_2\text{S}$  film (Chen et al., 2010; Martino et al., 2017). The copper transport first occurs as copper complexes and clusters, and eventually, all available sulphide is sequestered as  $\text{Cu}_2\text{S}$  (Chen et al., 2018; Smith, 2011). Further, at a constant concentration of  $\text{Cl}^-$ , the corrosion resistance of copper is decreased with increased sulphide concentration. Copper canisters are found mostly subject to general corrosion and an only minor degree of localised attack in the form of surface roughening. The roughening results in the formation of a porous and non-protective surface film with the supply of  $\text{HS}^-$  as the corrosion rate-determining factor (King and Lilja, 2014). Whereas, the conditions of high  $[\text{SH}^-]$  and  $\text{SH}^-$  flux that requested for the growth of partial passivate film supporting pitting are unachievable in the real repository conditions. Therefore, pitting corrosion of waste container surfaces should not occur in the real repository processes (Martino, 2018; Martino et al., 2019).

On the other hand, chloride ions impose several effects on the growth of the sulphide film: it displaces the adsorbed  $\text{SH}^-$ , makes the film porous, and at high chloride concentrations, facilitates the transportation of  $\text{Cu}^+$  into the solution. At a low concentration of sulphide, the protectiveness of the formed  $\text{Cu}_2\text{S}$  film is dependent on the amount of chlorides in the solution (Chen et al., 2017), and both the growth rate and porosity increases of the film with increasing  $[\text{Cl}^-]$  (Martino et al., 2017). The mechanism is that, at a high chloride/sulphide concentration ratio, the metal surface adsorbed  $\text{CuSH}$  species form soluble species ( $\text{CuCl}_n^{(n-1)-}$ ) via complexation reaction with  $\text{Cl}^-$ . The diffusion process of the soluble species would maintain the porosity in the base layer and limit the deposition of the outer protective  $\text{Cu}_2\text{S}$  deposit (Smith, 2011).

Further, the influence of bicarbonate ( $\text{HCO}_3^-$ ) anions has also been a concern on the stability of the copper oxide film. A literature survey and experimental work have been reported to clarify the issue. It is concluded that, although bicarbonate ions may threaten the Cu/anodic film system with high susceptibility to localized corrosion phenomena, bicarbonate ions alone are not likely to pose a serious hazard to the stability of copper oxide films on the shield of the canister (Sirkiä et al., 1999).

## **2.4 Literature review summary**

As a summary, from complimentary research results obtained from various scientific techniques and approaches with different concerns, it can be concluded that copper provides an excellent corrosion barrier in an underground repository (King et al., 2001). However, most of the experimental researches were using  $\text{Na}_2\text{S}$  as sulphide instead of  $\text{H}_2\text{S}$ , because of safety reasons for using  $\text{H}_2\text{S}$  in experiments. However,  $\text{H}_2\text{S}$  and  $\text{Na}_2\text{S}$  may have different dissociation behavior on Cu surface. In the case of  $\text{H}_2\text{S}$ , the atomic H may play an important role in the corrosion process, which is not the case for  $\text{Na}_2\text{S}$ . Moreover, in the reviewed literature, although possible chemical reactions are discussed, no thermodynamic calculation of the stable components (and their fraction) in the Cu-S- $\text{H}_2\text{O}$  and Cu-S-Cl- $\text{H}_2\text{O}$  systems has been reported.

Both research groups from KTH and VTT have been conducting researches on corrosion of copper nuclear waste canister for many years, and fruitful findings have been reported. General corrosion will not be an engineering problem in a repository since all the results present relatively low corrosion rates. Localization of the corrosion attack is one of concern. However, severe pitting of copper in groundwater has neither been observed from our previous researches nor has it been reported in the literature.

To achieve the utmost goal of final storage for the nuclear waste ‘in an absolutely safe way’ with a life of a hundred thousand to a million years, further collaborative efforts of both groups and with a broader extent will be made to better monitor the corrosion events and understand the related mechanisms. The future collaborative researches may be conducted with the special focuses of revealing the role of both H and S in the corrosion process of Cu, via carrying out the short- and long-term exposures of sulphide solutions and DFT calculation of the surface adsorption and reactions and their inward diffusion. The combination of the experimental and theoretical investigation will provide us with a throughout and deep understanding of the corrosion processes.

It should be easy to do that by using common data base, such as Medusa, from which one can calculate the equilibria of the system such as stability region and fraction of stable components as function of pH (and also electrode potential).

## **3. Materials and methods**

### **3.1 Materials**

Oxygen-free phosphorus-containing copper grade (OFP-Cu) was used as the material in these tests. Two initial conditions were used: (i) the ground copper surface and (ii) pre-oxidised copper surface, which was exposed to 90 °C temperature in air for seven days after grinding. The pre-oxidation is applied to simulate the effect of previous exposure to oxidic conditions on the copper material.

Three different sample types were used for different purposes. The electrochemical samples had an area of 1 cm<sup>2</sup>, they had the surface finish of 600 grit and were tested only with as-ground surfaces. For the mass loss measurements, coupons of approximately 70\*25\*(3-5) mm with surface finish of 600 grit were used. For characterisation purposes, samples with the dimensions of approximately 10\*10\*(3-5) mm with at least one surface polished to 1 µm were used. All samples were cleaned in acetone and ethanol prior to the test.

### 3.2 Exposure conditions

The exposure experiments were conducted at VTT. The samples were exposed to simulated groundwater with varied additions of sulphide. The chemical components (presented in Table 1) of the simulated groundwater are based on the groundwater of the disposal site with added bentonite effects. The sulphide addition was made by adding Na<sub>2</sub>S in the solution. The used sulphide concentrations are presented in Table 2. The tests were conducted at room temperature (22 °C). The test vessels were laboratory borosilicate gas tight glass bottles with volume of 2-5 L, depending on how many samples were in the bottle. The electrochemical samples were in their own bottles. The experiments were carried out in anoxic environment: the vessels were flushed with argon before initiating the test.

**Table 1.** The chemical components of the simulated groundwater.

	K	Ca	Cl	Na*	SO <sub>4</sub>	Br	HCO <sub>3</sub>	Mg	Sr	Si	B	F	Mn	PO <sub>4</sub>	lactate
mg/L	54.7	280.0	5274.0	3180.2	595.0	42.3	13.7	100.0	8.8	3.1	1.1	0.8	0.2	0.1	1

\*original Na addition; actual amount is dependent on the addition of Na<sub>2</sub>S

**Table 2.** Used sulphide additions and their corresponding concentrations.

Sulphide (S <sup>2-</sup> ) addition	Concentration of the solution
0 mg/L	0
3 mg/L	10 <sup>-4</sup> mol/L
32 mg/L	10 <sup>-3</sup> mol/L
320 mg/L	10 <sup>-2</sup> mol/L
640 mg/L	2*10 <sup>-2</sup> mol/L

The tests were run for four months (135 days). In addition, one test of two month (53 days) duration was conducted with 32 mg/L sulphide content to obtain some samples for characterisation at an earlier stage.

### 3.3 Methods

#### 3.3.1 Electrochemical methods

The samples were monitored with electrochemical measurements. Open circuit potential (OCP) and redox potential data was collected continuously throughout the test period. The used reference electrode was Ag/AgCl (anaerobic, 0.15 M KCl). A platinum electrode immersed in the vessels was used for redox measurements.

Linear polarization resistance (LPR), electrochemical impedance spectroscopy (EIS) and Tafel measurements were conducted once a week. Counter electrode was platinum and copper electrode was used as a working electrode and another as a reference electrode in these measurements. LPR measurement range was -20 to 20 mV vs. E<sub>OC</sub> with the rate of 0.16667 mV/s and Tafel from -30 to 30 mV vs. E<sub>OC</sub> with the rate of 0.16667 mV/s. The EIS was measured at OCP with 10 mV AC voltage, from 100000 to 0.001 Hz, eight points per

decade. The OCP measurements were conducted for 60 s at the start of these measurements. All the electrochemical measurements were performed using a Gamry Instruments potentiostat model Reference 600<sup>TM</sup> with DC105 and EIS300 software. Gamry Echem software was used to fit the Tafel and polarisation resistance plots.

The corrosion rate was calculated from the corrosion current in two different ways. The calculation of the corrosion rate (CR) is derived from the Faraday's law and according to ASTM standard G102-89 (ASTM, 1999) is calculated as:

$$CR = (i_{\text{corr}} * K * EW) / \rho$$

where  $i_{\text{corr}}$  is corrosion current density (corrosion current  $I_{\text{corr}}$  divided by the sample area),  $K$  is a constant depending on the wanted unit of the outcome,  $EW$  equivalent weight and  $\rho$  the density. For corrosion rates presented in mm/a, the constant  $K$  is 3272 mm/(A\*cm\*year) (Gamry, 2020).

In the first method, the  $I_{\text{corr}}$  is determined by using Tafel extrapolation. In the second calculation method,  $I_{\text{corr}}$  is calculated with the formula:

$$I_{\text{corr}} = (\beta_a * \beta_c) / (2.303 * R_p * (\beta_a + \beta_c))$$

where the  $\beta$  coefficients are obtained from the Tafel plots and the polarisation resistance ( $R_p$ ) from the linear polarisation curve (Gamry, 2020).

### 3.3.2 Microscopy

The samples were visually inspected and photographed. The surfaces were also examined with an optical stereomicroscope Leica MZ7.5.

Scanning electron microscope with field emission gun (FEGSEM) Zeiss UltraPlus Gemini was used for characterising the surfaces in more detail with both secondary electron (SE) and backscattered electron (BSE) modes. Moreover, energy dispersive X-ray spectroscopy (EDS) ThermoScientific UltraDry was used to obtain information on the chemical components present on the surfaces.

### 3.3.3 Water chemistry measurements

The water chemistry measurements were conducted at ALS Finland Oy with a number of analysis methods for different components of the solution. pH, alkalinity, conductivity, acidity, carbon dioxide and carbonates were determined with potentiometric titration (EN ISO 9963-1 and CSN 75 7373); Br, F, Cl and SO<sub>4</sub> with ion chromatography (ISO 10304-1, EN 16192); hydrogen sulphide and sulphide with spectrophotometry (CSN 83 0520-16, CSN 83 0530-31, SM 4500-S D); and B, Ca, Cu, Mg, Mn, K, Na, Si, Sr with inductively coupled plasma - mass spectrometry and atomic fluorescence spectroscopy (EPA 200.8, EN ISO 17294-2, EPA 6020A, EPA 245.7, EPA 1631, EN ISO 178 52, EN 16192).

### 3.3.4 High-energy X-ray diffraction (HEXRD)

The HEXRD measurements were carried out at the Swedish Materials Science beamline P21.2 at the synchrotron PETRA III at DESY, Hamburg, Germany. The photon energy was 96 keV (0.1291 Å) and the distance between the sample and the Varex 4343CT flat panel detector was about 1.6 m. LaB<sub>6</sub> was used for geometry calibration. The sample surface was

aligned to be parallel to the X-ray beam which was 20  $\mu\text{m}$  (vertical) times 55  $\mu\text{m}$  (horizontal) large. The entire specimen was scanned in 20  $\mu\text{m}$  steps across the entire specimen thickness. The 2D diffraction images were converted into 1D patterns using integrating the diffraction data along all azimuthal angles using pyFAI (Ashiotis et al., 2015). Recently, further synchrotron X-ray diffraction studies were conducted in grazing-incidence angles to collect information from samples exposed to 4 months in sulphide-containing solutions with varying concentrations (3-640 mg/l). The results will be documented in the next report.

### **3.3.5 Scanning Kelvin probe force microscopy (SKPFM)**

SKPFM was employed to measure the Volta potential difference (VPD) between tip (platinum) and the surface of the specimens with different exposure conditions. The Dimension Icon from Bruker with OSCM-Pt R3 probes from Olympus was used. The measurements were conducted in ambient air environment at 22°C and 23% relative humidity. The map resolution was 256 x 256 pixels. The nullifying bias was applied to the sample to show noble regions as high potentials, implying cathodic character, and less noble regions as low potentials, implying anodic character, in the Volta potential maps.

## **4. Results and discussion**

### **4.1 Electrochemical measurements**

The electrochemical measurements were conducted in designated bottles. The measurements across the duration of the test enable seeing the trends in corrosion throughout the test. The electrochemical measurements are still ongoing, and thus this section will present the preliminary corrosion rates calculated based on Tafel plot and LPR measurements. The EIS will be analysed at the end of the electrochemical experiment. These corrosion rates will be later compared to gravimetric results, which show the overall mass loss occurred during the test. Moreover, only at the end of the experiments can the samples, changes in water chemistry and other possibly affecting factors properly determined.

Figure 2a shows the progress of corrosion rates of samples exposed to solutions with 0, 32 and 320 mg/L sulphide additions when the corrosion current is extrapolated from Tafel plots. The average corrosion rate is overall the highest at the highest sulphide addition, but the rates at each point vary through the duration of the test. During the first approximately 11 days, the rate in sample with 0 mg/L increases initially, but after that decreases to less than 2  $\mu\text{m/a}$ . However, there is a very small increase across the time.

In the sample exposed to 32 mg/L, in turn, the rate varies slightly until approximately 70 days, at which the rate is increased. After this jump, the rate is low, even less than 1  $\mu\text{m/a}$ , but it then increases after 120 days of duration. The sample in the 320 mg/L sulphide solution shows an increase across the duration, generally having the highest corrosion rate. The corrosion rates calculated based on the LPR measurements (in Figure 2b) confirm the trends.

Figure 2c presents the open circuit potential (OCP) and redox measurements from the same experiments of 0, 32 and 320 mg/L. For the 32 mg/L experiment, there appears to be a distinct change at approximately 70 days: the OCP increases significantly. This is also seen in the corrosion rates presented in Figure 2a and b. One possibility for the reason of this could be that at this point the sulphide in the water has been used up in the reactions, and thus it ceases to react with the material, consequently increasing the OCP of the sample. Other, smaller jump in the 32 mg/L experiment was seen after 120 days, which corresponds

to the increase of corrosion rate. Moreover, in OCP of the 0 mg/L sample, there is a jump after 20 days. This corresponds with the time period, after which the corrosion rates seem to be more even in that sample.

Considering the data from the first shorter test, with the duration of 53 days in 32 mg/L solution, it can be seen that the rate is rather stable, but a notable change occurs at 70 days: this highlights the need for longer tests to complement the measurements in unexpected changes.

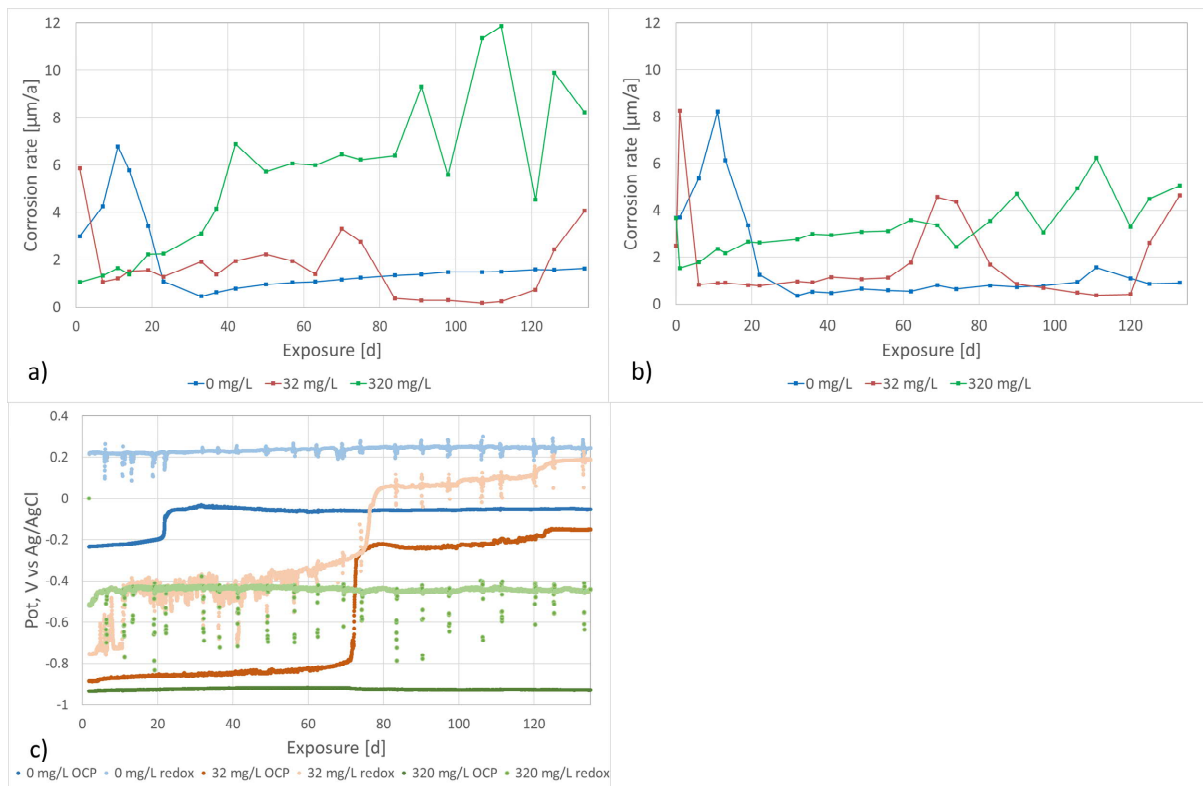


**Figure 2.** Electrochemical measurement results of the samples in solutions with 0, 32 and 320 mg/L sulphide addition as a) corrosion rates calculated with the  $I_{\text{corr}}$  determined by extrapolating from Tafel plots, b) corrosion rates calculated based on LPR measurements and c) open circuit potential and redox measurements.

## 4.2 Surface characterisation: 2 month tests

In the following sections, first all the surface characterisations are presented for the samples after two month exposure, including the visual/optical observations, scanning electron microscopy, high-energy X-ray diffraction observations and scanning Kelvin probe force microscopy.

### 4.2.1 Visual observations

Photographs before and after the two month exposure have been gathered to Figure 3. The figure shows the samples in both ground and pre-oxidised states, as well as both sides of the samples after the exposure. It can be seen that after the exposure, both ground and pre-oxidised samples appear rather similar. They both are clearly more oxidised than before exposure.

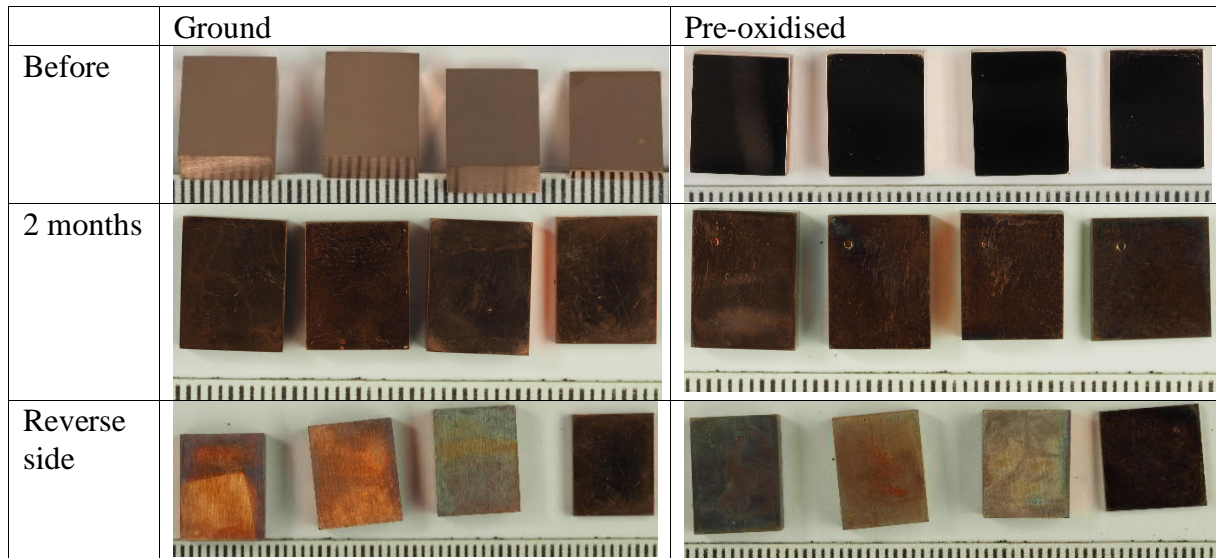
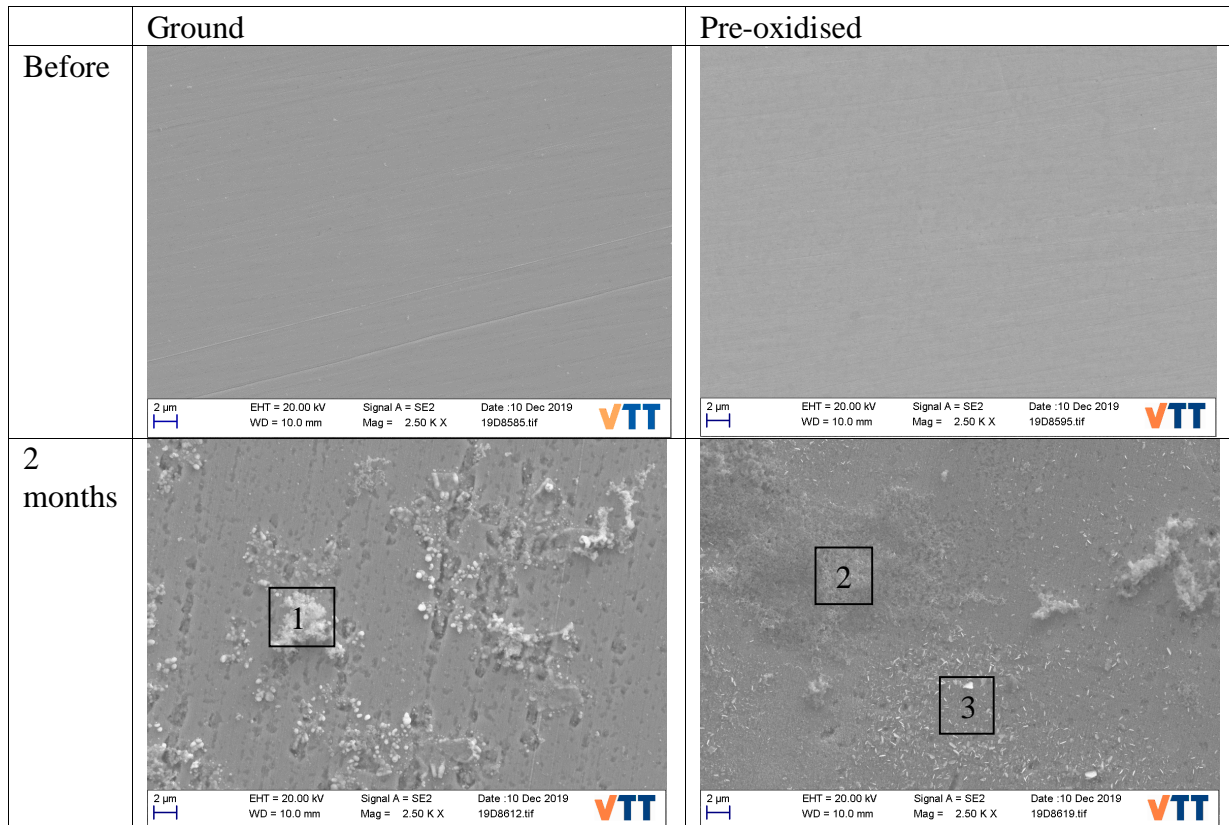


**Figure 3.** Photographs of the characterisation samples before and after the 2 month exposure in 320 mg/L sulphide solution. Length of the sample is approximately 10 mm; one gap in the scale bar is 1 mm. Tilting of the sample may affect the appearance of the colour.

However, it is also noteworthy that there are rather large differences between the individual samples and their two sides. This is deemed to originate from the positioning of the samples, as at times some surfaces may face the vessel bottom or another sample, which may limit its exposure to the solution.

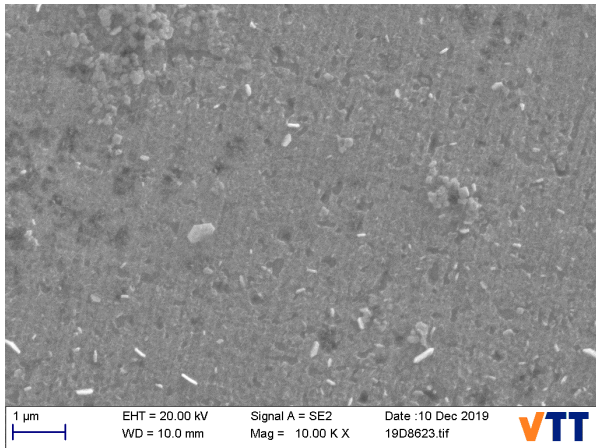
#### 4.2.2 SEM observations

Having a closer look at the surfaces after the 2 month exposure with SEM, it was observed that there were recessions and also deposits in both ground and pre-oxidised samples. Figure 4 presents the SEM images of ground and pre-oxidised samples before and after the exposure. For the surfaces before the exposure, there was only a very small difference between the ground and pre-oxidised surfaces. The presence of oxides was suggested by very faint shapes visible on the surface. The EDS analysis confirmed there to be more oxygen on the pre-oxidised sample (approximately 2 at% on the pre-oxidised in comparison to less than 1 at% in the ground sample).



**Figure 4.** SEM images of ground and pre-oxidised samples before and after 2 month exposure.

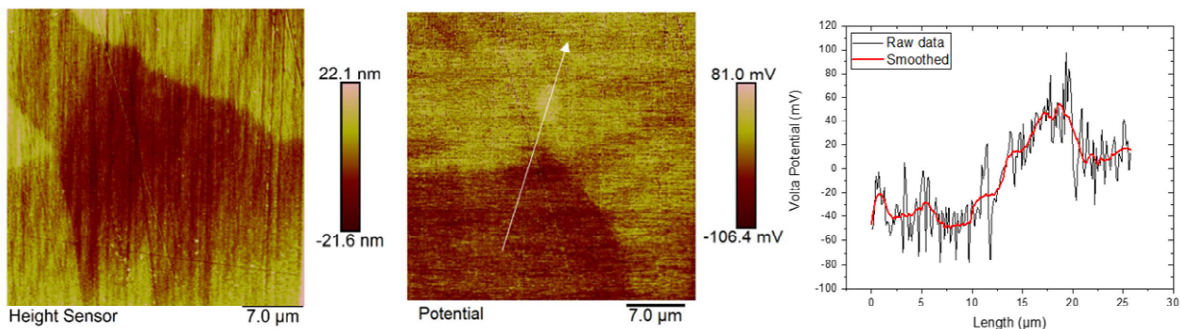
The exposed samples appear distinctly different from their initial states: recessions ranging from submicron to a couple of micrometre scale could be seen on the surface, as seen in Figure 4. There are also different kinds of deposits on the exposed surfaces. A bit larger, light contrast deposits (such as location 1 marked in Figure 4) were found to have a significant amount of oxygen (in excess of 25 at%) and also varying amounts of magnesium, silicon and carbon - however, with carbon it must be remembered that with especially light elements, EDS is not very accurate. Also other kinds of deposits or products were found in the studied locations of the pre-oxidised sample, as marked with locations 2 and 3 in Figure 4. The area marked with “2” had the main elements of oxygen and sulphur, with some calcium and carbon as well. The area marked with “3” had whisker-shaped and angular-shaped products on it. Figure 5 presents a close-up of these products. An EDX of an area containing a flake had more sulphur than the surrounding area.



**Figure 5.** A close-up SEM image of a pre-oxidised sample after 2 month exposure.

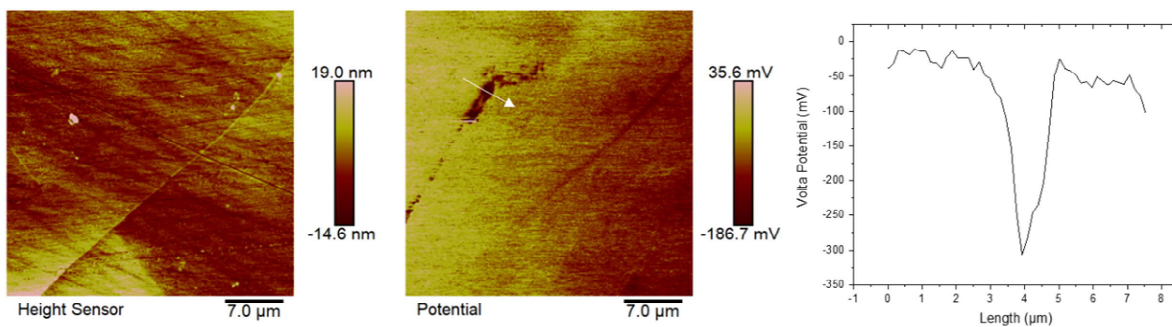
#### 4.2.3 Scanning Kelvin probe force microscopy

Figure 6 shows the results of the VPD measurements carried out on the non-exposed specimens. The obtained pattern in the topography map did not match with the measured Volta potential information. There is a distinctive anodic and cathodic site visible in the potential map having a potential difference of up to 100 mV suggesting these as grains with different orientation. Grains with varying crystallographic orientation can have different work functions, hence, different Volta potentials due to different surface energy.



**Figure 6.** Topography (left) and Volta potential (middle) maps of the non-exposed, ground and polished specimen. The profile (right) shows extracted Volta potential information along the line shown in the potential map.

The results for the specimen oxidized at 90°C for 7 days are summarized in Figure 7. There, grain boundaries can be seen to protrude slightly the surface with parts having anodic and cathodic Volta potentials. Moreover, speckled contrast in the potential map was observed. This region had no distinctive topographic feature. A line profile was extracted across this site, as shown in Figure 7 (right), showing a VPD of up to 250 mV relative to the neighbouring matrix.



**Figure 7:** Topography (left) and Volta potential (middle) maps of the non-exposed, ground and polished, and pre-oxidised specimen at 90°C for 7 days. The profile (right) shows extracted Volta potential information along the line shown in the potential map.

The results for the specimen exposed to 32 mg/L sulphur for 53 days is summarized in Figure 8. The surface was full of nanometre-sized recessions and spherical protrusions. The recessed sites showed anodic Volta potentials circa 50 mV lower than the matrix whereas the protrusions were cathodic approximately 50 mV higher than the neighbouring matrix.

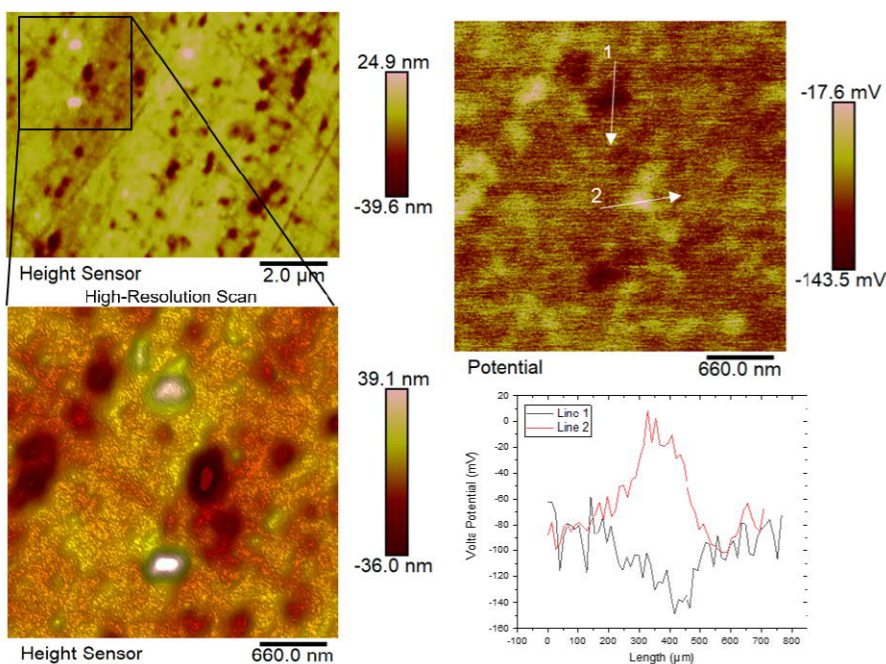


**Figure 8:** Topography (left) and Volta potential (right) maps of the specimen ground and polished and then exposed to 32 mg/L S for 53 days. The profile (right) shows extracted Volta potential information along the line shown in the potential map.

#### 4.2.4 High-energy X-ray diffraction

The HEXRD measurements revealed structural changes on the near-surface and bulk microstructure of the copper samples. The diffraction results are briefly summarised in Figure 9. The analysis of the data from the surface region (Figure 9, upper diagrams) suggest that the pre-oxidation led to formation of amorphous oxide products of two different kinds. After the exposure to sulphide-containing electrolyte (32 mg/L, 53 days), the surface contained corrosion products, mainly copper sulphide-compounds with a certain crystalline nature. One surface oxide compound, formed during pre-oxidation, seemed to have dissolved during the exposure to the electrolyte. The synchrotron technique also enabled measurement of the

strains in the material. Large macrostrains (up to 0.12%) were measured in the copper bulk after the exposure to the electrolyte, suggesting the infusion of hydrogen as well as sulphur. The strain developed in the copper is two orders of magnitude higher than those caused by hydrogen in stainless steels (data from earlier work on stainless steel), which suggests that infusion of sulphur has occurred. However, further analysis is needed to confirm the infusion of sulphur into copper.

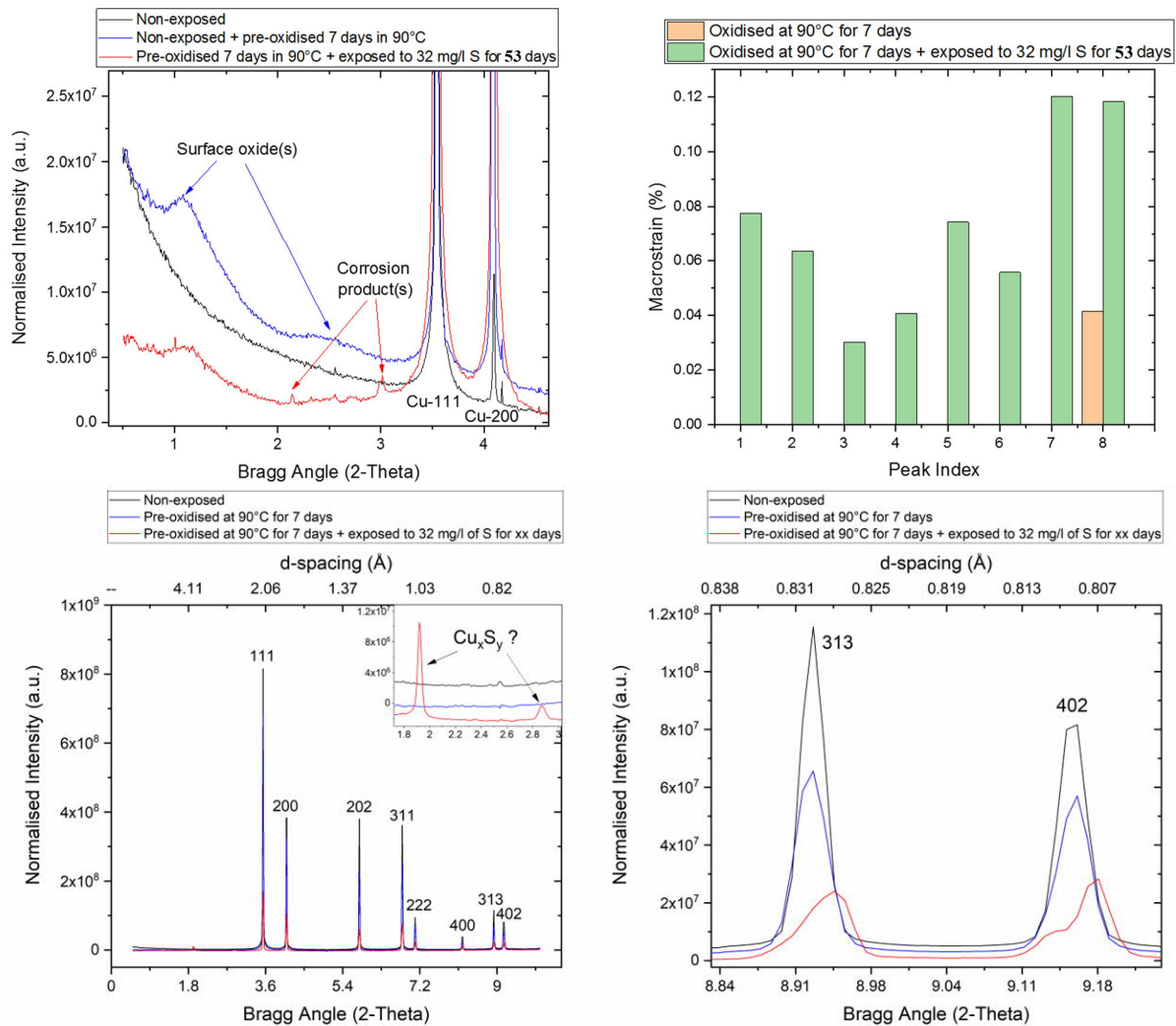


**Figure 9:** Summary of High-energy X-ray diffraction results.

Overall, viewed from the diffraction data of whole sample (Figure 9, lower diagrams), the results show that the exposure to the sulphide-containing solution led to clear shifts of all peaks suggesting changes of the copper crystal lattice. The peaks, furthermore, widened and showed peak splitting which indicates the evolution of large lattice stresses in the microstructure. Moreover, diffraction signals of copper sulphide compounds are evident. More detailed work will be conducted to improve understanding of microstructure and surface properties of the exposed specimens.

### 4.3 Surface characterisation: 4 month tests

#### 4.3.1 Visual observations

When the bottles were observed after the four-month exposure, some of them had a sediment on the bottom of the bottle, covering the samples. This sediment was seen in bottles with

sulphide content of 32 mg/L and above, whereas the bottle with solution of 3 mg/L seemed to have clear contents. Figure 10 presents the bottles after four months of exposure test, before the setup was disassembled.

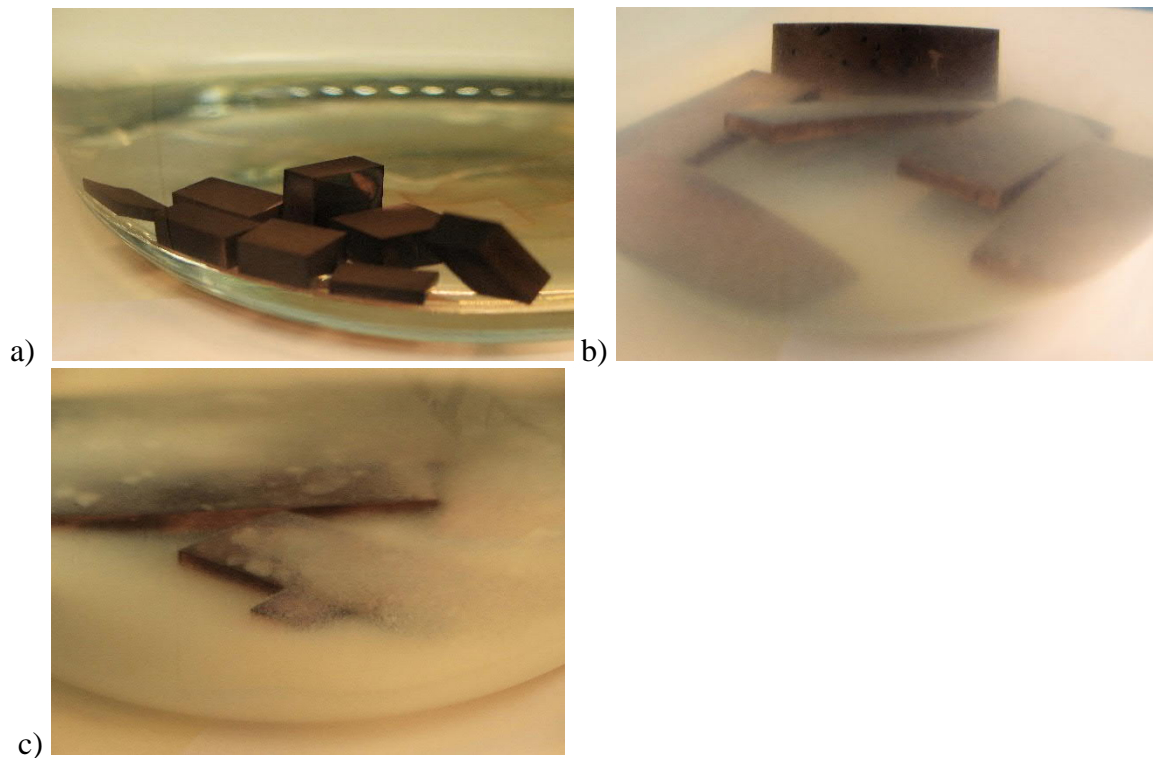


**Figure 10.** Samples in the bottles after four month exposure, the solution having the sulphide addition of a) 3 mg/L, b) 32 mg/L and c) 640 mg/L.

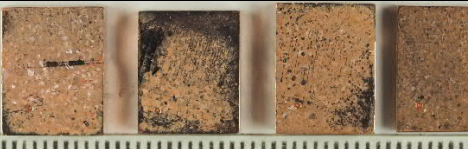
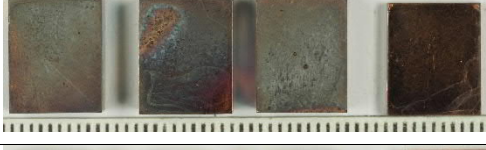
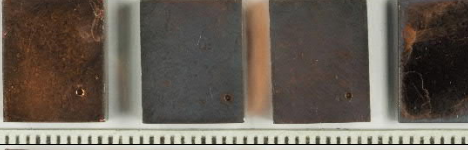
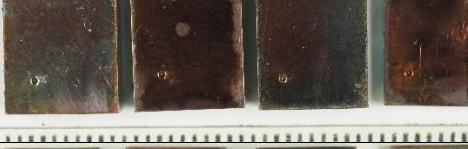
Another practical matter which was noticed was that in some cases, the added  $\text{Na}_2\text{S}$  (solid granules) had not dissolved quickly enough but had landed on some of the samples, causing the appearance of the areas where the granules hit to be distinctly different from the general areas, such as in Figure 11 where a 32 mg/L sample is shown. This was the most noticeable in samples in the 32 mg/L sulphide solution.



**Figure 11.** Ground sample after four month exposure in solution with sulphide addition of 32 mg/L. Gaps in scale bar 1 mm.

Figure 12 shows the photographs of the characterisation samples after four month exposure in solutions with varied sulphide levels. At times the individual samples are rather different from one another within the same sulphide level, level of discolouration varying between the samples. Some overall trends can be seen, though. The samples exposed to only simulated

groundwater (0 mg/L) are distinctly different from those exposed to sulphide solutions. They have remained mostly of metallic colour, but exposure to water has revealed the grain structure. This revelation of the grain structure occurs also in sulphide solutions, but is less apparent due to the formation of surface films. Usually the ground, non-pre-oxidised surfaces show the grain structure somewhat better, possibly due to the thinner initial oxide layer.

Sulphide addition	Ground	Pre-oxidised
not exposed		
0 mg/L		
3 mg/L		
32 mg/L		
320 mg/L		
640 mg/L		

**Figure 12.** Photographs of the characterisation samples before and after the 4 month exposure. Length of the sample is approximately 10 mm; one gap in the scale bar is 1 mm. Tilting of the sample may affect the appearance of the colour.

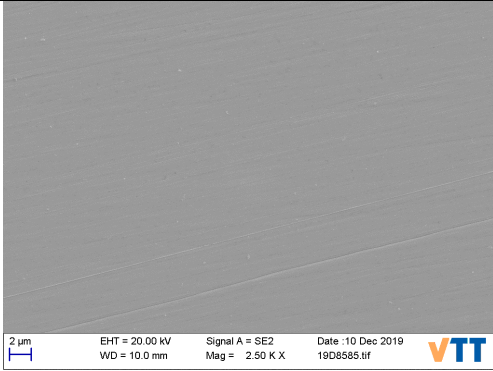
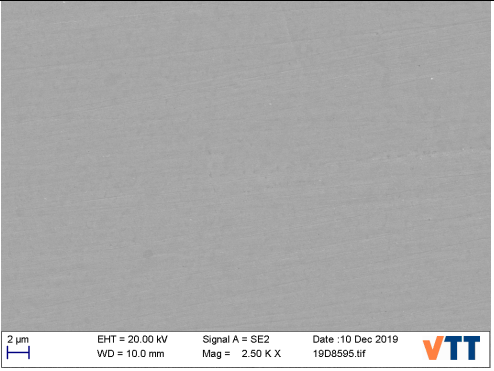
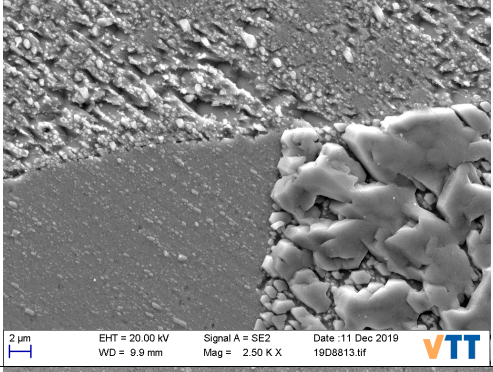
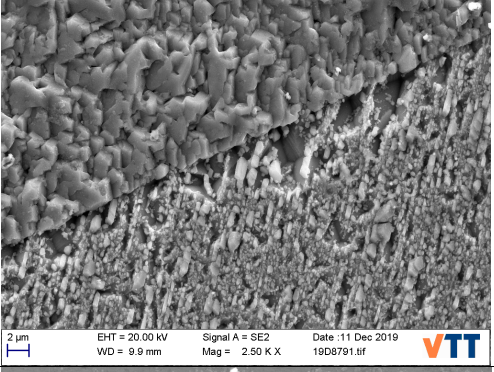
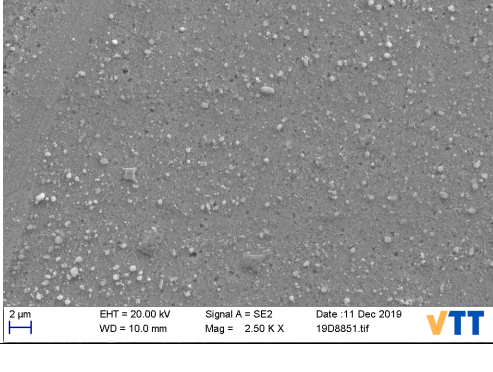
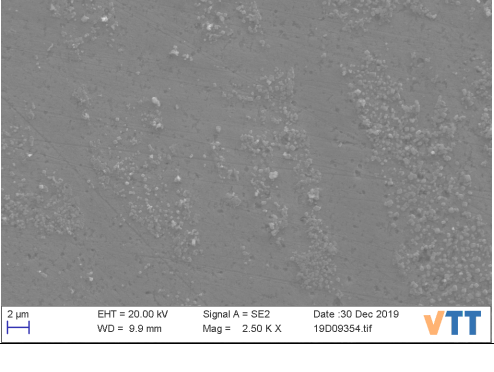
#### 4.3.2 SEM observations

The following section describes the general observations of the 4 month samples. Like seen in the visual observations, there were local differences within the sample surfaces and the corrosion product coverage is not uniform throughout all the surfaces. In all of the cases, throughout the whole sulphide addition range, the exposed surfaces were clearly affected. In most of the polished (down to 1  $\mu\text{m}$ ) samples, differences between the behaviour of different grains could be observed, suggesting a difference of tendency in corroding depending on the orientation of the grain.

In the samples having been exposed to simulated groundwater without sulphide addition (0 mg/L), the corrosion product crystals were detected to be copper oxide (most possibly  $\text{Cu}_2\text{O}$ ) by EDS. It also shows a clear difference in the oxide growth between the grains and the grain boundaries appear to be attacked, as seen in Figure 13.

As a general observation, the samples exposed to water with sulphide additions had depressions on the surface already at the lowest addition (3 mg/L). Locally, the surface could be having relatively large depressions already at the lowest sulphide addition, as seen in Figure 14.

The samples exposed to water with sulphide additions had crystals on the surface which are rich in sulphur and copper, indicating them to be copper sulphides. However, EDS reveals that also oxygen remained on the surface, and other compounds might be present. For example, in the 320 mg/L samples, also calcium oxides were presumably on the surface. It is possible that Raman spectroscopy, which is being done, will shed more light on the compounds.

Sulphide addition	Ground	Pre-oxidised
not exposed		
0 mg/L		
3 mg/L		

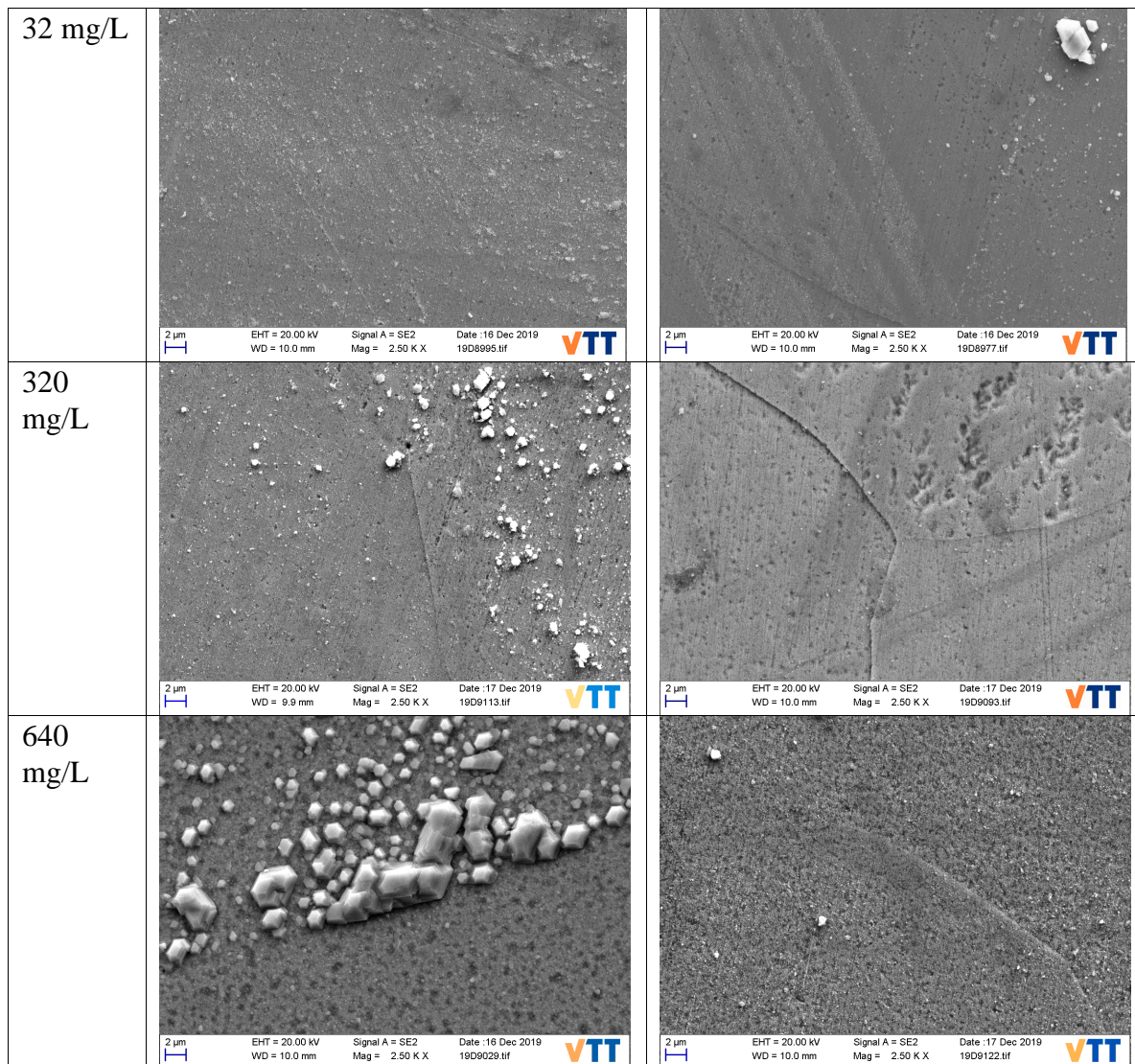


**Figure 13.** SEM images of the polished samples exposed to the simulated ground water with varied amounts of sulphide addition.

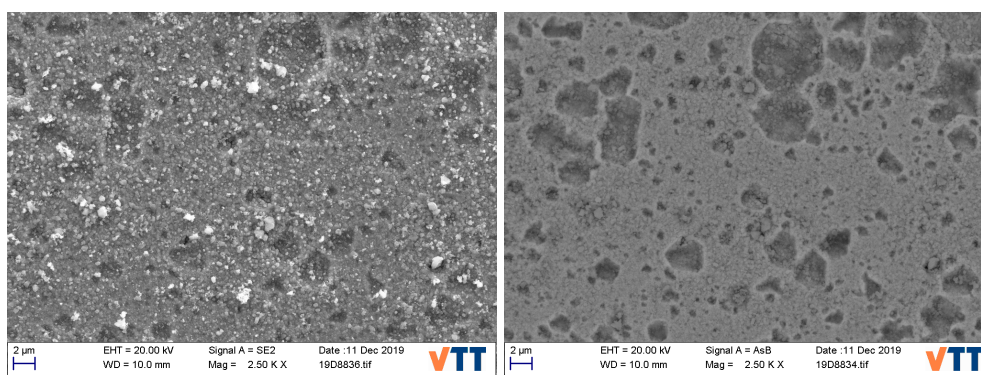


**Figure 14.** An SEM image of a pre-oxidised polished sample exposed to simulated groundwater with 3 mg/L sulphide addition: secondary electron image (left), backscattered electron image (right).

#### 4.4 Water analysis

The water chemistries of the characterisation sample bottles were measured after the test and the results are presented in Table 3. For reference, the calculated amounts of each component from the simulated groundwater are presented on the right hand side, as well as a note of the

overall trend in regards to the increasing sulphide content. There are some irregularities in the trends, especially in the 32 mg/L ( $10^{-3}$  mol/L) sample, which was slightly out of trends, but the values were mostly within the error ranges. However, one irregularity was clearly larger than the error ranges: the amount of sulphide in the 32 mg/L sample was more than double than what it was based on the sulphide addition.

Copper seems to dissolve with the sulphide content of 0-3 mg/L ( $0-10^{-4}$  mol/L), whereas above this sulphide concentration the detected amount of copper in the solution was less than 10  $\mu$ g/L. So at lower sulphide levels, there appears to be more dissolution of copper. Moreover, the added sulphide seems to have been used completely in the reactions within the 4 month exposure in the bottle where the addition was 3 mg/L, as the sulphide level in this samples was <0.05 mg/L. In other words, there was lack of sulphide in solution at the end of the test. Another difference between the waters was that the amount of hydrocarbonates in solution is increased approximately ten-fold in each ten-fold increase of the sulphide addition. It was also observed that the magnesium and manganese concentrations decrease in the highest sulphide addition level 320-640 mg/L ( $10^{-2}$  mol/L -  $2 \cdot 10^{-2}$  mol/L) samples to only a fraction from the original values.

It was also observed that the amount of boron is clearly increased when the addition of sulphide is at the level of 32 mg/L ( $10^{-3}$  mol/L) or above, and its concentration significantly surpasses the level added to the simulated groundwater. As there are no other known sources of boron in the simulated groundwater, this raises a suspicion of there being a possibility of reaction with the borosilicate container material (which includes  $\text{SiO}_2$  and  $\text{B}_2\text{O}_3$ ). In addition to this, there are irregularities in the amount of soluble silicon in the water samples with 320-640 mg/L ( $10^{-2}$  and  $2 \cdot 10^{-2}$  mol/L) sulphide addition levels: in 320 mg/L ( $10^{-2}$  mol/L), the concentration of silicon is approximately half of the levels observed at lower sulphide addition levels where the silicon concentration remains at the level of the simulated groundwater (3.1 mg/L). In the 640 mg/L ( $2 \cdot 10^{-2}$  mol/L) sample, there was approximately 1.7 times more silicon than in the original solution. This high amount of silicon backs up the suspicion of there possibly being a reaction between the solution and the container.

Comparing the water with no sulphide addition to the waters with varied levels of sulphide, the water sample without sulphide addition showed elevated amount of carbon dioxide, whereas in all other of the studied samples the amount of carbon dioxide was below the detection limit. Another clear difference between the water sample with no sulphide addition to the samples with the addition was the significantly decreased amount of strontium. In the water without the sulphide addition, the strontium levels had decreased to the levels of approximately 0.08 mg/L, in the other samples the levels being at their original expected level (100 times higher, around 8.8 mg/L).

**Table 3.** Water chemistries after the tests. On the right hand side, the original values of the simulated groundwater components are presented as well as the overall observed trends. Values presented in red refer to the value of the tested water being higher than the calculated values of that component in the simulated groundwater. Values highlighted in yellow refer to the value being distinctly different from the values measured from the other waters.

Component	Unit	0 mg/L	3 mg/L	32 mg/L	320 mg/L	640 mg/L	Simulated groundwater (calculated)	Trend
pH		7.66	8.37	8.88	10.6	11.7		increasing
conductivity	mS/m	1640	1660	1650	1750	1970		increasing
bromide	mg/L	31.7	31.3	27.2	31.4	31.2	42.3	stable (irregular)
fluoride	mg/L	0.682	<1.00	0.582	<1.00	<1.00	0.8	stable
carbonates (CO <sub>3</sub> <sup>2-</sup> )	mg/L	0.00	2.50	8.26	72.7	81.6		increasing
chloride	mg/L	4780	4660	4050	4630	4630	5274	stable (irregular)
hydrogen sulphide	mg/L	<0.050	<0.050	79.4	181	250		increasing
sulphate	mg/L	448	430	392	428	444	595	stable (irregular)
sulphide	mg/L	<0.050	<0.050	74.7	170	235	0/3/32/320/640	increasing
acidity, pH 8.3	mmol/L	<0.150	<0.150	<0.150	<0.150	<0.150		stable
hydrocarbonates (HCO <sub>3</sub> <sup>-</sup> )	mg/L	8.74	4.59	42.3	443	1040	13.7	increasing (irregular)
carbon dioxide, all	mg/L	8.11	5.14	36.5	373	813		increasing (irregular)
acidity, pH 4.5	mmol/L	<0.150	<0.150	<0.150	<0.150	<0.150		stable
carbon dioxide, free	mg/L	1.80	0.00	0.00	0.00	0.00		(irregular)
aggressive carbon dioxide	mg/L	1.80	0.00	0.00	0.00	0.00		(irregular)
alkalinity, pH 4.5	mmol/L	<0.150	0.158	0.968	9.68	19.8		increasing
alkalinity, pH 8.3	mmol/L	<0.150	<0.150	<0.150	1.21	1.36		increasing
Cu, all	µg/L	207	66.1	<10.0	<10.0	<10.0		decreasing
Soluble metals:								
B	µg/L	958	925	1460	2680	3060	1100	increasing
Ca	µg/L	261000	255000	271000	252000	221000	280000	stable (irregular)
Cu	µg/L	167	63.9	<10.0	<10.0	<10.0		decreasing
K	µg/L	49700	49200	49200	49900	49000	54700	stable
Mg	µg/L	80500	80800	72800	855	67.6	100000	decreasing
Mn	µg/L	104	86.0	6.68	<1.00	<1.00	200	decreasing
Na	µg/L	2720000	2910000	2760000	3180000	3420000	3180200-	
Si	mg/L	2.98	3.10	3.01	1.43	5.39	3.1	increasing? (irregular)
Sr	mg/L	0.0757	8.64	8.65	8.42	8.54	8.8	stable (irregular)

#### 4.4.1 Proposition for further tests to find the source of additional silicon and boron

For the integrity of the corrosion results, some additional tests are proposed to be run to clarify if there is a reaction between the borosilicate container material and the used solution. Now the findings of there being significantly more boron and silicon soluble in the water than originally indicate that this might be happening. Moreover, there is a distinct sediment being formed in the exposure bottles when the solution has 32 mg/L or more of sulphide added.

The alternative source of additional silicon is the usage of silicon carbide papers to grind the samples to the required surface finish. However, this procedure is the same for all samples in all the bottles. Moreover, this does not account for the increased boron levels, which were up to more than 2.5 times the original additions in the simulated groundwater.

According to chemical resistivity tables (Bürkle GmbH, 2020), FEP and PTFE would be resistant to the sulphide-added water. However, they are not gas tight (Gas permeability of fluoropolymers [sic], 2020), which is an essential requirement when conducting experiments in anoxic conditions.

Optimally, it would be interesting to test different materials (such as glass and fluoropolymer) at different levels of sulphide additions and durations of exposure to observe their suitability for periods of extended exposure. Moreover, it would be interesting to compare the effects of a simplified water (only sulphide and chloride added) with the sulphide-added simulated groundwater, which has several different ions. The primary outcome of additional tests would be to verify a proper vessel material for the long-term copper experiments in sulphide-containing environment. Secondary outcome would be to contribute to the ongoing long-term corrosion studies on copper and other materials in relevant final repository conditions and point out possible sources of errors or uncertainties.

#### **4.5 Selecting the parameters for the next experiments**

One of the goals of this project was to study the influence of different ions on the corrosion of copper in sulphide-containing environment. King and Lilja (2014) conclude based on collecting several different references that the most important ion species regarding the pitting of copper are  $\text{Cl}^-$ ,  $\text{SO}_4^{2-}$  and  $\text{HCO}_3^-$ : increasing amount of  $\text{HCO}_3^-$  promotes passivation, whereas  $\text{Cl}^-$  and  $\text{SO}_4^{2-}$  are promoting the breakdown of the film. They also state that the amount of  $\text{HCO}_3^-$  plays a role in how the other ions affect the pitting potential.

There already are some studies available on how especially chloride affects the formation of the film on the surface of copper in these conditions (Chen et al., 2017; Martino et al., 2014; Martino et al., 2017; Smith et al. 2011), and it has been concluded that the film morphology is affected by the presence of higher values of chloride. The used parameters of studies on the effect of sulphide or/and chloride on corrosion of copper are presented in Table 4. However, many of these tests have been conducted in Type I water, which is very pure, with sulphide and chloride additions. In real groundwater, there are many other components present, such as sulphate and metallic ions.

This, together with the fact that the corrosion of *pre-oxidised* copper in real groundwater has not been widely studied, makes the case of assessing the effect of chloride levels on the forming surface film. Thus it can be determined if changes in the chloride level change also the resulting film after oxidation. In our previous study (Isotahdon et al., 2019), it was found that pre-oxidation of copper increased the mass loss after the exposure in abiotic anoxic simulated groundwater for 252 days at 37 °C. Smith et al. (Smith et al., 2007a; Smith et al., 2007b) studied the films on the samples and tested the corrosion potentials of pre-oxidised copper in sulphide and chloride containing solution. They determined that the oxide layer is converted to sulphide at all tested sulphide levels ( $10^{-5}$  to  $10^{-3}$  mol/L). However, the pre-oxidation of the samples was conducted electrochemically, and the used solution was a very simplified version in comparison to real conditions, which makes it important to have another look into the film formation of pre-oxidised copper in conditions simulating the real

conditions more closely. The adjusting of the chloride content will be conducted through looking at reported groundwater compositions and also estimated compositions at the time point of above 10 000 years after closure to find the lowest and highest estimated levels present in long-term storage.

**Table 4.** Parameters used in selected studies on the effect of sulphide or/and chloride ions on the corrosion of copper.

Na <sub>2</sub> S [mol/L]	Cl [mol/L]	Duration	Ref.
10 <sup>-3</sup>	0.1 NaCl	8 h	Hollmark et al., 2012
5*10 <sup>-5</sup>	0.1 NaCl	4000 h (~167 days)	Chen et al., 2011
5*10 <sup>-4</sup>	0.1 NaCl		Chen et al., 2018
10 <sup>-3</sup>	0.1 to 5.0	1691 h (~71 days)	Chen et al., 2017
10 <sup>-4</sup> to 10 <sup>-3</sup>	0.1 NaCl		Martino et al., 2019
10 <sup>-5</sup> to 2*10 <sup>-3</sup>	0.1-5.0		Martino et al., 2017
10 <sup>-5</sup> to 10 <sup>-2</sup>	0.1 NaCl	~400 min + 9 days	Smith et al., 2007c
10 <sup>-3</sup>	0.1-5.0 NaCl	30 h	Smith et al., 2011
3*10 <sup>-5</sup> to 10 <sup>-3</sup>	0.1 NaCl	55 h	Smith et al., 2007
5*10 <sup>-5</sup> to 5*10 <sup>-2</sup>	0.1 NaCl	3600s	Kong et al., 2017
5*10 <sup>-5</sup> to 2*10 <sup>-3</sup>	0.1-5 NaCl		Martino et al., 2014
10 <sup>-5</sup> to 10 <sup>-3</sup>	0.1 NaCl	80 h	Smith et al., 2007b

In the case of sulphate, it is believed that the sulphate-reducing bacteria will transform sulphate into sulphide (Pedersen, 2000). Martino (2018) has run some tests with sulphates, and King and Lilja (2014) have drawn together results also with sulphate containing solutions.

The amount of Cl<sup>-</sup>, SO<sub>4</sub><sup>2-</sup> and HCO<sub>3</sub><sup>-</sup> in the simulated groundwater are presented in Table 5 along with the maximum values predicted to be present in the repository after extended period of time (more than 10 000 years) in (King et al., 2001). When comparing the amount of the ions, it seems that the chloride content of the current study is well in line with most of the predicted repository site groundwater compositions presented here (in Olkiluoto, the Cl<sup>-</sup> content higher than at other sites). The effect of higher chloride content will be tested by adding more Cl<sup>-</sup> in one of the tests. Similarly, the sulphate content is rather well in line with most of the sites, as is the bicarbonate. But as the nature of bicarbonate is different than the chloride and sulphate, bicarbonate was selected as another ion to be varied.

**Table 5.** The amount of specific ions in the simulated groundwater and the maximum values predicted to be present in the repository after more than 10 000 years. The three top rows refer to the amount of ions present in the waters and the three bottom rows the ratios [mol/mol] of the ions in each water. Simpevarp, Forsmark and Olkiluoto values are from King et al., 2001.

Ions	Simulated groundwater [mg/L]	Simulated groundwater [mol/L]	Simpevarp [mol/L]	Forsmark [mol/L]	Olkiluoto [mol/L]
Cl <sup>-</sup>	5274.0	0.1488	0.1400	0.1400	0.4200
SO <sub>4</sub> <sup>2-</sup>	595.0	0.0062	0.0042	0.0042	0.0052
HCO <sup>3-</sup>	13.7	0.0002	0.0004	0.0007	N/A
Cl <sup>-</sup> / SO <sub>4</sub> <sup>2-</sup>		24.0	33.3	33.3	N/A
Cl <sup>-</sup> / HCO <sup>3-</sup>		662.6	350.0	200.0	N/A
SO <sub>4</sub> <sup>2-</sup> / HCO <sup>3-</sup>		27.6	10.5	6.0	N/A

## 5 Summary and conclusions

OFP-copper samples were exposed to anoxic simulated groundwater with varying amounts of sulphide addition (0-640 mg/L) to study the effect of the presence of sulphides in simulated repository conditions. Copper samples in two states were used: in ground/polished state and pre-oxidised state (7 days, 90 °C in air). The duration of exposure was 4 months in these experiments, to get initial results aiding the selection of experimental parameters for the longer term experiments later. In addition to this, an experiment with the exposure duration of 2 months was conducted. Several characterisation methods were used: visual examination, scanning electron microscopy and energy dispersive X-ray spectroscopy, scanning Kelvin probe force microscopy and high-energy X-ray diffraction. Moreover, electrochemical data was collected throughout the experiment.

The results indicate that the addition of sulphide in the simulated groundwater has a distinct effect on copper. The surfaces were affected already at the lowest addition level (3 mg/L), however there was local variance in the surfaces. The electrochemical measurements suggested that the corrosion was the highest with higher sulphide addition (320 mg/L was the highest electrochemically measured sample). Open circuit potentials of the samples were the lower, the higher the addition of sulphide was.

Main preliminary conclusion from the synchrotron XRD measurement was that in addition to the copper sulfide compounds formed on the surface, the exposure also induced the structural change of the surface region of copper, which may increase the susceptibility to cracking under mechanical stress. Further measurement and analysis of H and S ingress into the copper are needed to draw a safe conclusion.

The water measurements indicated that there may be a reaction between the simulated groundwater with added sulphide and the vessel, and this needs to be considered before the next experiment. As the next steps, the longer term experiments are set up, and the further/more detailed characterisation of the samples continues.

## Acknowledgments

NKS conveys its gratitude to all organizations and persons who by means of financial support or contributions in kind have made the work presented in this report possible.

Taru Lehtikuusi, Tuomo Kinnunen, Marketta Mattila, Seija Kivi and Mervi Somervuori are gratefully acknowledged for their assistance with the experiments at VTT. Vuokko Heino is thanked for SEM and EDS analysis.

### **Disclaimer**

The views expressed in this document remain the responsibility of the author(s) and do not necessarily reflect those of NKS. In particular, neither NKS nor any other organisation or body supporting NKS activities can be held responsible for the material presented in this report.

### **6 References**

- Andersson, C, Rinne, M, Staub, I & Wanne, T. 2004. The on-going pillar stability experiment at the Äspö hard rock laboratory, Sweden. In: Stephanson, O. (Ed.). Elsevier Geo-Engineering Book Series 2. Elsevier. pp. 389-394.
- Ashiotis, G, Deschildre, A, Nawaz, Z, Wright, JP, Karkoulis, D, Picca, FE & Kieffer, J. 2015. The fast azimuthal integration Python library: pyFAI. *Journal of Applied Crystallography*. 48: 510-519.
- ASTM, 1999. G 102-89 (Reapproved 1999) Standard practice for calculation of corrosion rates and related information from electrochemical measurements. ASTM, pp. 429-435.
- Bennett, DG & Gens, R. 2008. Overview of European concepts for high-level waste and spent fuel disposal with special reference waste container corrosion. *Journal of Nuclear Materials* 379: 1-8.
- Bo, R, Pan, J & Leygraf, C. 2005. Tafel slopes used in monitoring of copper corrosion in a bentonite/groundwater environment. *Corrosion Science*. 47: 3267-3279.
- Bo, R & Pan, J. 2008. An electrochemical impedance spectroscopy study of copper in a bentonite/saline groundwater environment. *Electrochimica Acta*. 53: 7556-7564.
- Bo, R, Kosec, T, Kranjc, A, Pan, J & Legat, A. 2011. Electrochemical impedance spectroscopy of pure copper exposed in bentonite under oxic conditions. *Electrochimica Acta*. 56: 7862-7870.
- Bürkle GmbH. 2020. Chemical resistance. Version 3.6. 22 p.
- Carpén, L, Rajala, P & Bomberg, M. 2016. Microbially induced corrosion of copper in simulated anoxic groundwater. In: *Proceedings of Eurocorr 2016*. 11 p.
- Carpén, L, Rajala, P, Huttunen-Saarivirta, E & Bomberg, M. 2017. Corrosion Behavior of Copper in Simulated Anoxic Groundwater Inoculated with Sulfate Reducing Bacteria and Methanogens. In: *CORROSION 2017. NACE*. pp. 3686-3700.
- Carpén, L, Rajala, P & Bomberg, M. 2018. Corrosion of Copper in Anoxic Ground Water in the Presence of SRB. *Corrosion Science and Technology*. 17: 147-153.
- Chen, J, Qin, Z & Shoesmith, D. 2010. Kinetics of corrosion film growth on copper in neutral chloride solutions containing small concentrations of sulfide. *Journal of the Electrochemical Society*. 157: C338-C345.
- Chen, J, Qin, Z & Shoesmith, D. 2011. Long-term corrosion of copper in a dilute anaerobic sulfide solution. *Electrochimica Acta*. 56: 7854-7861.
- Chen, J, Qin, Z & Shoesmith, D. 2014. Key parameters determining structure and properties of sulphide films formed on copper corroding in anoxic sulphide solutions. *Corrosion Engineering, Science and Technology*. 49: 415-419.
- Chen, J, Qin, Z, Martino, T & Shoesmith, D. 2017. Effect of chloride on Cu corrosion in anaerobic sulphide solutions. *Corrosion Engineering, Science and Technology* 52: 40-44.

Chen, J, Qin, Z, Martino, T, Guo, M & Shoesmith, D. 2018. Copper transport and sulphide sequestration during copper corrosion in anaerobic aqueous sulphide solutions. *Corrosion Science*. 131: 245-251.

Cragolino, GA & Sridhar, N. 1991. Localized Corrosion of a Candidate Container Material for High-Level Nuclear Waste Disposal. *Corrosion*. 47: 464-472.

Cragolino, GA, Dunn, DS, Pan, YM & Pensado, O. 2011. Corrosion Processes Affecting the Performance of Alloy 22 as a High-Level Radioactive Waste Container Material. *MRS Proceedings*. 663: 507.

DoE. 2002. A Technology Roadmap for Generation IV Nuclear Energy Systems.

Foxt, F & Gras, JM. 2003. Semi-empirical model for carbon steel corrosion in long term geological nuclear waste disposal. In: *Prediction of Long Term Corrosion Behaviour in Nuclear Waste Systems*. pp. 91-102.

Gamry. Accessed 2020. Getting Started with Electrochemical Corrosion Measurement - Review of the Electrochemical Basis of Corrosion. Available at: <https://www.gamry.com/application-notes/corrosion-coatings/basics-of-electrochemical-corrosion-measurements/>.

Gas permeability of fluoropolymers [sic]. Accessed 2020. Available at: [https://archive-resources.coleparmer.com/Manual\\_pdfs/01410-10Permeability.pdf](https://archive-resources.coleparmer.com/Manual_pdfs/01410-10Permeability.pdf).

He, X, Ahn, T & Gwo, JP. 2018. Corrosion of Copper as a Nuclear Waste Container Material in Simulated Anoxic Granitic Groundwater. *Corrosion*. 74: 158-168.

Hedman, T, Nyström, A & Thegerström, C. 2002. Swedish containers for disposal of spent nuclear fuel and radioactive waste. *Comptes Rendus Physique*. 3: 903-913.

Hellä, P, Pitkänen, P, Löfman, J, Partamies, S, Vuorinen, U & Wersin, P. 2014. Safety Case for the Disposal of Spent Nuclear Fuel at Olkiluoto - Definition of Reference and Bounding Groundwaters, Buffer and Backfill Porewaters. Posiva. 171 p.

Hollmark, H, Keech, P, Vegelius, J, Werme, L & Duda, LC. 2012. X-ray absorption spectroscopy of electrochemically oxidized Cu exposed to Na<sub>2</sub>S. *Corrosion Science*. 54: 85-89.

Huttunen-Saarivirta, E, Rajala, P & Carpén, L. 2016. Corrosion behaviour of copper under biotic and abiotic conditions in anoxic ground water: electrochemical study. *Electrochimica Acta*. 203: 350-365.

Huttunen-Saarivirta, E, Rajala, P, Bomberg, M & Carpén, L. 2017a. Corrosion of copper in oxygen-deficient groundwater with and without deep bedrock micro-organisms: Characterisation of microbial communities and surface processes. *Applied Surface Science*. 396: 1044-1057.

Huttunen-Saarivirta, E, Rajala, P, Bomberg, M & Carpén, L. 2017b. EIS study on aerobic corrosion of copper in ground water: influence of micro-organisms. *Electrochimica Acta*. 240: 163-174.

Huttunen-Saarivirta, E, Ghanbari, E, Mao, F, Rajala, P, Carpén, L & Macdonald, DD. 2018. Kinetic Properties of the Passive Film on Copper in the Presence of Sulfate-Reducing Bacteria. *Journal of The Electrochemical Society*. 165: C450-C460.

Ikeda, BM, Bailey, MG, Quinn, MJ & Shoesmith, DW. 1994. The Development of an Experimental Data Base for the Lifetime Predictions of Titanium Nuclear Waste Containers. In: Cragolino, G & N. Sridhar, N (Eds.). *Application of Accelerated Corrosion Tests to Service Life Prediction of Materials*. PA: ASTM International. pp. 126-142.

Isotahdon, E, Carpén, L & Rajala, P. 2019. Corrosion of copper in geological repository for nuclear waste - The effect of oxidic phase on the corrosion behaviour of copper in anoxic environment. In: *Proceedings of EUROCORR 2019*. 8 p.

Karnland, O & Sandén, T. 1999. Long-Term Test of Buffer Material at ASPO Hard Rock Laboratory, Sweden. MRS Online Proceeding Library Archive. 608: 173.

King, F, Ahonen, L, Taxén, C, Vuorinen, U & Werme, L. 2001. Copper corrosion under expected conditions in a deep geologic repository. Swedish Nuclear Fuel and Waste Management Co.

King, F, Lilja, C, Pedersen, K, Pitkänen, P & Vähänen, M. 2010. An update of the state-of-the-art report on the corrosion of copper under expected conditions in a deep geologic repository. Swedish Nuclear Fuel and Waste Management Co.

King, F & Lilja, C. 2014. Localised corrosion of copper canisters. Corrosion engineering, science and technology. 49: 420-424.

King, F & Kolar, M. 2018. Lifetime Predictions for Nuclear Waste Disposal Containers. Corrosion. 75: 309-323.

Kong, D, Dong, C, Xu, A, Man, C, He, C & Li, X. 2017. Effect of sulfide concentration on copper corrosion in anoxic chloride-containing solutions. Journal of Materials Engineering and Performance. 26: 1741-1750.

Kursten, B, Smailos, E, Azkarate, I, Werme, L, Smart, NR & Santarini, G. 2004. COBECOMA. State of the art document on the Corrosion Behaviour of Container Materials. European Commission. 299 p.

Mao, F, Dong, C, Sharifi-Asl, S, Lu, P & Macdonald, DD. 2014. Passivity breakdown on copper: Influence of chloride ion. Electrochimica Acta. 144: 391-399.

Marja-aho, M, Rajala, P, Huttunen-Saarivirta, E, Legat, A, Kranjc, A, Kosec, T, Carpén, L. 2018. Copper corrosion monitoring by electrical resistance probes in anoxic groundwater environment in the presence and absence of sulfate reducing bacteria. Sensors and Actuators A: Physical. 274: 252-261.

Martino, T, Partovi-Nia, R, Chen, J, Qin, Z & Shoesmith, DW. 2014. Mechanisms of film growth on copper in aqueous solutions containing sulphide and chloride under voltammetric conditions. Electrochimica Acta. 127: 439-447.

Martino, T, Chen, J, Qin, Z & Shoesmith, DW. 2017. The kinetics of film growth and their influence on the susceptibility to pitting of copper in aqueous sulphide solutions. Corrosion Engineering, Science and Technology 52: 61-64.

Martino, TL. 2018. Electrochemical and Corrosion Examination of Copper under Deep Geologic Conditions for the Application of Nuclear Waste Containers. The University of Western Ontario.

Martino, T, Smith, J, Chen, J, Qin, Z, Noël, J & Shoesmith, D. 2019. The Properties of Electrochemically-Grown Copper Sulfide Films. Journal of The Electrochemical Society. 166: C9-C18.

Pedersen, K. 2000. Microbial processes in radioactive waste disposal, SKB Swedish Nuclear Fuel and Waste Management Co. Technical Report, TR-00-04. SKB. 98 p.

Rosborg, B, Eden, D, Karnland, O, Pan, J & Werme, L. 2003. The Corrosion Rate of Copper in a Test Parcel at the Äspö Hard Rock Laboratory. Mrs Proceedings. 807: 489.

Rosborg, B, Eden, DA, Karnland, O, Pan, J & Werme, LO. 2004. Real-Time Monitoring of Copper Corrosion at the Aspo Hard Rock Laboratory.

Scully, JR & Edwards, M. 2013. Review of the NWMO copper corrosion allowance. Nuclear Waste Management Organization.

Shoesmith, DW, Ikeda, BM & King, F. 1994. Modelling Procedures for Predicting the Lifetimes of Nuclear Waste Containers. In: Trethewey, KR & Roberge, PR (Eds.). Modelling Aqueous Corrosion: From Individual Pits to System Management. Springer Netherlands. pp. 201-238.

- Sirkiä, P, Saario, T, Mäkelä, K, Laitinen, T & Bojinov, M. 1999. Electric and electrochemical properties of surface films formed on copper in the presence of bicarbonate anions. *Radiation and Nuclear Safety Authority*. 22 p.
- Smart, NR, Reddy, B, Rance, AP, Nixon, DJ, Frutschi, M, Bernier-Latmani, R, et al. 2017. The anaerobic corrosion of carbon steel in compacted bentonite exposed to natural Opalinus Clay porewater containing native microbial populations. *Corrosion Engineering, Science and Technology*. 52: 101-112.
- Smith, J, Wren, J, Odziemkowski, M & Shoesmith, D. 2007. The electrochemical response of preoxidized copper in aqueous sulfide solutions. *Journal of the Electrochemical Society*. 154: C431-C438.
- Smith, JM, Qin, Z, Wren, JC & Shoesmith, DW. 2007b. The influence of preoxidation on the corrosion of copper nuclear waste canisters in aqueous anoxic sulphide solutions. *MRS Proceedings*. 985: 301–306.
- Smith, J, Qin, Z, King, F, Werme, L & Shoesmith, DW. 2007c. Sulfide film formation on copper under electrochemical and natural corrosion conditions. *Corrosion*. 63: 135–144.
- Smith, JM, Qin, Z, King, F & Shoesmith, DW. 2011. The influence of chloride on the corrosion of copper in aqueous sulfide solutions. In: Fèron, D et al. (Eds.). *Sulphur-Assisted Corrosion in Nuclear Disposal Systems: (EFC 59)*. Maney Publishing. pp. 109–123.
- Sridhar, N & Cragnolino, G. 1993. Applicability of Repassivation Potential for Long-Term Prediction of Localized Corrosion of Alloy 825 and Type 316L Stainless Steel. *Corrosion*. 49: 885-894.
- Wang Ju, ZT. 2003. Ten years progress of the radioactive waste disposal. *The International Progress* 7. 476-480.

Title	Corrosion of copper in sulphide containing environment: the role and properties of sulphide films - Annual report 2019
Author(s)	Vilma Ratia <sup>1</sup> , Leena Carpen <sup>1</sup> , Elisa Isotahdon <sup>1</sup> Cem Örnek <sup>2</sup> , Fan Zhang <sup>2</sup> , Jinshan Pan <sup>2</sup>
Affiliation(s)	<sup>1</sup> VTT Technical Research Centre of Finland Ltd., Espoo, Finland <sup>2</sup> KTH Royal Institute of Technology, Stockholm, Sweden
ISBN	978-87-7893-524-3
Date	April 2020
Project	NKS-R / COCOS
No. of pages	33
No. of tables	5
No. of illustrations	14
No. of references	58

Abstract  
max. 2000 characters

OFP-copper samples were exposed to anoxic simulated groundwater with varying amounts of sulphide addition (0-640 mg/L) to study the effect of the presence of sulphides in simulated repository conditions. Copper samples in two states were used: in ground/polished state and pre-oxidised state (7 days, 90 °C in air). The duration of exposure was 4 months in these experiments, to get initial results aiding the selection of experimental parameters for the longer term experiments later. In addition to this, an experiment with the exposure duration of 2 months was conducted. Several characterisation methods were used: visual examination, scanning electron microscopy and energy dispersive X-ray spectroscopy, scanning Kelvin probe force microscopy and high-energy X-ray diffraction. Moreover, electrochemical data was collected throughout the experiment.

The results indicate that the addition of sulphide in the simulated groundwater has a distinct effect on copper. The surfaces were affected already at the lowest addition level (3 mg/L), however there was local variance in the surfaces. The electrochemical measurements suggested that the corrosion was the highest with higher sulphide addition (320 mg/L was the highest electrochemically measured sample). Open circuit potentials of the samples were the lower, the higher the addition of sulphide was.

Main preliminary conclusion from the synchrotron XRD

measurement was that in addition to the copper sulfide compounds formed on the surface, the exposure also induced the structural change of the surface region of copper, which may increase the susceptibility to cracking under mechanical stress. Further measurement and analysis of H and S ingress into the copper are needed to draw a safe conclusion.

The water measurements indicated that there may be a reaction between the simulated groundwater with added sulphide and the vessel, and this needs to be considered before the next experiment. As the next steps, the longer term experiments are set up, and the further/more detailed characterisation of the samples continues.

Key words

corrosion, copper, nuclear waste, sulphide, characterisation